July 2015

RNAi Mediated Silencing of Cell Wall Invertase Inhibitors to Increase Sucrose Allocation to Sink Tissues in Transgenic Camelina Sativa Engineered with a Carbon Concentrating Mechanism

Joshua Zuber
University of Massachusetts Amherst

RNAi Mediated Silencing of Cell Wall Invertase Inhibitors to Increase Sucrose Allocation to Sink Tissues in Transgenic *Camelina Sativa* Engineered with a Carbon Concentrating Mechanism

A Thesis Presented

By

JOSHUA ZUBER

Submitted to the Graduate School of the

University of Massachusetts Amherst in partial fulfillment

of the requirements for the degree of

Master of Science

May 2015

Biochemistry and Molecular Biology

RNAi Mediated Silencing of Cell Wall Invertase Inhibitors to Increase Sucrose Allocation to Sink Tissues in Transgenic *Camelina Sativa* Engineered with a Carbon Concentrating Mechanism

A Thesis Presented

By

JOSHUA ZUBER

Approved as to style and content by

_____

Danny J. Schnell, Chair

_____

Om Parkash, Member

_____

Jennifer Normanly, Department Head

Biochemisty and Molecular Biology

DEDICATION

To my family and friends for their love and support,
I could not have done this without you

ACKNOWLEDGEMENTS

I would like to acknowledge the many lab members I have had the pleasure of working with over my academic career in Danny Schnell's Lab. I have learned more in the laboratory than I could have possibly dreamed of when I first came in for an interview as a freshman undergraduate. I learned a great deal from then post-doc Hitoshi Inoue, and it is in part by his influence that I believe resulted in my success in the laboratory. I have found the best way to learn and to teach is by example, and neither was ever of short supply in the Schnell Laboratory.

Without the guidance of Danny J. Schnell, none of this would have been possible. Danny has supported me throughout my laboratory career both in my academic and personal life. The consideration he has shown me is immense, and for that I am very grateful.

In closing I would like to acknowledge those that have assisted me in completion of my thesis work for a Master of Science degree. This includes my committee members, Danny Schnell and Om Parkash, and post-doctoral fellow, Bibin Paulose, for their assistance in conducting experiments and writing this thesis. Lab members Cindy Nguyen, Lorenz Manker, and Kenny Ablordeppey also assisted me throughout the project.

ABSTRACT

RNAI MEDIATED SILENCING OF CELL WALL INVERTASE INHIBITORS TO INCREASE SUCROSE ALLOCATION TO SINK TISSUES IN TRANSGENIC *CAMELINA SATIVA* ENGINEERED WITH A CARBON CONCENTRATING MECHANISM

MAY 2015

JOSHUA ZUBER, B.S., UNIVERSITY OF MASSACHUSETTS AMHERST

M.S., UNIVERSITY OF MASSACHUSETTS AMHERST

Directed by: Professor Danny J. Schnell

Plant invertases are a class of proteins that have enzymatic function in cleaving sucrose to fructose and glucose. Cell wall invertase, located on the exterior of the cell wall of plant cells, plays a key role in the unloading of sucrose from the apoplast to the sink tissues. Cell wall invertase interacts with an inhibitor, cell wall invertase inhibitor, post-transcriptionally to regulate its activity. The inhibitor is constitutively expressed in pollen development, early developing seeds, and senescing leaves: indicative of sucrose allocation being a limiting factor at these stages of development. We introduced algal bicarbonate transporters LCIA/CCP1 to *Camelina sativa* for the purpose of increasing photosynthetic capacity. The bicarbonate transporters concentrate CO_2 at RuBisCO by pumping CO_2 in the form of bicarbonate through the membrane, then converting it back to CO_2 at RuBisCO, increasing CO_2 concentration. Results from these plants have shown an increase in seed number, but not seed mass, along with a faster rate of maturity and senescence. This is indicative of acclimation to high CO_2 conditions, resulting from insertion of the bicarbonate transporters. RNA sequencing was performed and a putative

invertase inhibitor was recognized as being expressed in the transgenic *C. sativa* but not in the wild type. Our strategy is to knock out two invertase inhibitors using induced RNA silencing, dramatically altering sucrose allocation into developing seeds and resulting in an increase in seed biomass. It is the aim of this research to increase the biomass of *C. sativa* seeds in order to increase its effectiveness as an agent to create sustainable biofuels.

TABLE OF CONTENTS

LIST OF TABLES

LIST OF FIGURES

CHAPTER 1

1 INTRODUCTION

1.1 Decreasing Carbon Emissions With Biofuels

Climate change poses a serious threat to plant and animal life on Earth for future generations (Maclean & Wilson, 2011; Thomas et al., 2004). It is now agreed upon that increased greenhouse gas emissions, such as CO_2, are the primary cause of the rapid climate change Earth is currently experiencing (Change, 1996; Ledley et al., 1999). In an effort to combat this, the United States government has recently made it a goal to decrease greenhouse gas emissions by 30% of the 2005 levels by 2030 (Davenport, 2014). Fossil fuel use accounts for the vast majority of greenhouse gas emissions (Marland, Boden, Andres, Brenkert, & Johnston, 2003). Therefore, reducing fossil fuel consumption will significantly decrease emissions overall. In recent years, bio-based fuel has emerged as a viable option for use in internal combustion engines, in place of traditional fuels (Agusdinata, Zhao, Ileleji, & DeLaurentis, 2011; X. Li & Mupondwa, 2014). Bio-based fuel is a carbon-based combustible liquid created from either (1) the seed oils of a variety of plants including corn, canola, and sunflower or (2) cellulosic plants such as grasses. *Camelina sativa*, a plant related to canola, has emerged as a popular seed oil-derived biofuel-dedicated crop due to its low-agronomic requirements and high seed yield (Putnam, Budin, Field, & Breene, 1993).

1.2 *Camelina Sativa* as a Dedicated Biofuel Crop

1.2.1 *Camelina Sativa*: A Low-Input Oilseed

C. sativa, also known as "False-flax" or "Gold-of-Pleasure", is a member of the Brassicaceae family and has traditionally been cultivated as an oilseed crop in Europe and Asia. Today it is viewed as a next-generation biofuel-producing crop for North America due to its' large seed yield and high oil content (~40%) (Kagale et al., 2014). *C. sativa* has the advantage of a short growing season (85-100 days seed to seed), low moisture requirements, adapted cold-tolerance, and resistance to many pathogens and pests (Putnam et al., 1993). Due to its vigor, and payback in seed for use in biofuel, it has developed into a popular "fallow-land" planting rotation for farmers. Through crop rotation of renewable energy producing *C. sativa* with feedstocks such as wheat or corn, confliction with food production space is avoided, while still alleviating monoculture practice (Shonnard, Williams, & Kalnes, 2010). By using *C. sativa* as a fallow-land crop in place of other traditional crops such as rye, the farmer gains income from growing a renewable energy-producing crop that has market value, in combination with giving benefits to the soil for future agricultural use and production.

1.2.2 *Camelina Sativa* Biofuel is Effective in Aviation

The Department of Defense is the country's largest energy consumer and is dedicated to exploring renewable energy options to meet greenhouse gas emission goals. The United States Navy currently blends 50% of its jet-fuel with *C. sativa*-based biofuel in order to decrease overall fuel costs and limit fossil fuel use by the U.S. government (X. Li & Mupondwa, 2014). This 50% mixture is the upper-level approved for use, as combustion engines require 25% aromatic compounds and current bio-refinery processes

are not capable of production at that level. Incorporating traditional fossil fuel raises the aromatic content of the biofuel to meet aviation standards. Tests on this fuel mixture show a reduction of CO_2 greenhouse gas emissions of up to 75% (Shonnard et al., 2010).

Current methods of creating biofuel from seed-based oil are relatively costly and inefficient compared to the well-adopted methods of fossil fuel extraction (Hill, Nelson, Tilman, Polasky, & Tiffany, 2006). Extensive research is being conducted to create better and cheaper methods for seed oil extraction and biofuel creation, however the timeline and feasibility of these projects is unclear. By utilizing the technology we currently have developed for biofuel creation, it is still possible to decrease overall costs and increase biofuel output. This can be done by increasing the amount of seed material output per plant, or by increasing the percentage of the oil component in the seed.

1.3 Increasing Oilseed Yield For Biofuels

1.3.1 Factors Affecting Yield

Factors affecting yield have been well established since early studies by Monteith (Monteith & Moss, 1977). The yield potential of a crop is expressed as a relationship between the amount of primary production (P_n) of a crop and the ability of said crop to appropriate energy to harvestable tissues at maturity (η), also known as the harvest index or partitioning efficiency (Long, ZHU, Naidu, & Ort, 2006). The primary production of a crop is a function of the total incident solar radiation (S_t), light interception efficiency (ε_i), and light conversion efficiency (ε_c). These equations are shown below in Table 1.

Symbols	Expressions
Y_p = Yield Potential η = Harvest Index	Yield Potential: $Y_p = \eta \cdot P_n$ Primary Production: $P_n = S_t \cdot \varepsilon_i \cdot \varepsilon_c / k$

P_n = Primary Production S_t= Total Incident Solar Radiation ε_i= Light Interception Efficiency ε_c= Light Conversion Efficiency k=Energy Content of Biomass	

Table 1: Monteith Yield Relationship Expressions

According to the expressions shown in Table 1, yield potential is calculated through the product of primary production and partitioning efficiency to harvestable biomass. Therefore, increasing partitioning efficiency will likewise increase yield potential to the same degree. Over the last 50 years, partitioning efficiency has mostly been exploited over primary production as a target for the realization of improved yield potential. For this reason, it is expected that few breakthroughs in factors affecting harvest index will be made in the future to increase yield potential.

Primary production has mostly sought improvements through improvements to the light interception efficiency (Zhu, Long, & Ort, 2010). Light interception efficiency is determined by factors of the leaf canopy, including rate of development, overall size, and architecture. Improvements have been made to the light interception efficiency through earlier canopy development time and increased ground cover. Like the harvest index, the light interception efficiency does not show a promising outlook for future improvements. This leaves light conversion efficiency as the remaining prospect for increasing yield potential in oilseed crops.

The light conversion efficiency of a plant is determined by the efficiency that light energy is converted to biomass by photosynthesis. Due to inefficiencies in enzymes responsible for photosynthesis, a competing respiration reaction results frequently in most plants. This results in decreased light conversion efficiency and a decrease in yield

potential through decreased primary production. For this reason, the light conversion efficiency has been a desirable target for improvements to increase yield potential. An increase in light conversion efficiency is coincident with improvements to photosynthesis rate relative to respiration rate. For this reason improvements to photosynthesis have the greatest potential for increasing yield potential in oilseed crops in the future.

1.3.2 Seed Oil & Yield Depends on Products of Photosynthesis

Oil and fats, along with proteins and carbohydrates, are a major component of all seeds. These components all depend on sucrose derived from photosynthesis for their synthesis (Rolland, Baena-Gonzalez, & Sheen, 2006). The light harvesting reaction of photosynthesis drives the conversion of light energy to chemical energy, and, in the presence of CO_2 and H_2O, drives the creation of sucrose. Photosynthesis levels are highest in mature green leaf tissue, which is the "source" of the created carbon-based sugar, sucrose. Sucrose needs to be transported from the "source" tissue, where it was synthesized, to non-photosynthetic "sink" tissues, such as root and floral tissues, to provide cellular energy for growth and function.

Sucrose is transported from the source tissue through the cell wall and into the phloem and companion cell complex. It is then transported via bulk-flow to the sink tissues, and unloaded via the cell-wall apoplasm or plasmodesmata (Koch, 2004). The sucrose feeds reactions that synthesize triacylglycerols (TAGs), starch, and proteins. The TAGs are the desired end product for use in bio-fuel production. There are a variety of approaches possible to attempt to increase available TAG seed oil. One major approach is to increase the overall output of sucrose from photosynthesis. Increasing sucrose

trafficking to sink tissues will increase the availability of substrate for the enzymes in the TAG-synthesis pathway.

1.4 Photosynthetic Carbon Capture Limits Yield

1.4.1 Inefficiency of RuBisCO

Photosynthesis depends largely on the enzymatic function of Ribulose-1, 5-Bisphosphate Carboxylase/Oxygenase (RuBisCO), which is responsible for fixing carbon to Ribulose-1,5-Bisphosphate (RuBP) as part of the Calvin Cycle. Due to its carboxylase/oxygenase nature, RuBisCO is responsible for catalyzing two competing reactions: carboxylation and oxygenation. Carboxylation is responsible for fixing carbon, and oxygenation is responsible for fixing oxygen, to RuBP. RuBisCO has a natural affinity for CO_2 but fixes O_2 to RuBP in approximately 25% of all reactions (Ellis, 2010a).

Carboxylated RuBP creates 3-phosphoglycerate (3-PGA), which is available for use in the Calvin-Benson Cycle to create cellular energy in the form of ATP. Energy production through this process is called C_3 photosynthesis. Oxygenated RuBP creates 2-phosphoglycolate (2-PGA) and 3-PGA as part of a process called photorespiration. The 3PGA created in the reaction is available for use in the Calvin-Benson Cycle for ATP production, whereas 2-PGA undergoes a complex set of reactions to reenter the Calvin-Benson Cycle, called C_2 photosynthesis. Although C_2 photosynthesis does produce ATP, it accounts for a 25% loss of available atmospheric CO_2. C_2 Photosynthesis also uses ATP in the process of photorespiration to generate 3-PGA, resulting in a net loss of energy. C_2 photosynthesis for this matter is not an efficient process for ATP production.

Because RuBisCO fixes O_2 in 25% of reactions there is flux between both C_2 and C_3 photosynthesis. Most vascular plants fix carbon through these mechanisms.

1.4.2 Improving Catalytic Efficiency of RuBisCO

RuBisCO accounts for over 50% of soluble leaf protein in C_3 plants, and 30% in C_4 plants, making it the most abundant protein overall (Ellis, 1979). RuBisCO has a relatively slow enzymatic rate, fixing only 3-10 molecules of CO_2 per second, making it a desirable target for improving the output of photosynthesis (Ellis, 2010b; Spreitzer & Salvucci, 2002). For many years attempts at increasing the affinity of RuBisCO for CO_2 has been largely unsuccessful, along with attempts at increasing the overall amount of RuBisCO in the leaves by overexpression (Spreitzer & Salvucci, 2002). Recent research, however, has exhibited an increased photosynthetic output of tobacco plants engineered with RuBisCO of cyanobacterial origin (Lin, Occhialini, Andralojc, Parry, & Hanson, 2014). This finding has exciting implications for future use in agriculture for both food and renewable energy production.

1.4.3 C_4 and CAM Plants' Evolved Anatomy for Increased Carbon Capture

A sub-set of plants, called C_4 and "Crassulacean Acid Metabolism" (CAM) plants, have evolved mechanisms to limit the damage of photorespiration by isolating RuBisCO from oxygen and providing only CO_2. These plants evolved the ability to separate the light-harvesting and carbon dioxide-harvesting events by conducting them at separate times of day and/or using a distinct leaf anatomy. The day/night plants, called CAM plants, evolved in arid conditions to limit water loss by collecting atmospheric CO_2 through open stomata during the night when temperatures are cool and RuBisCO is not present, and closing stomata during the day when temperatures cause increased

transpiration and photorespiration. The collected atmospheric CO_2 is stored as four-carbon malate in the vacuoles of leaf mesophyll cells, and is released during the day to provide CO_2 to RuBisCO for the light harvesting reaction—while limiting stomatal opening and water loss due to transpiration.

C_4 plants make use of their evolved leaf anatomy that contains photosynthetic chloroplasts in both mesophyll and bundle sheath cells, in contrast to only having photosynthetic capacity in mesophyll cells of C_3 and CAM plants. It is speculated that these plants may have evolved during a time when the atmosphere of Earth was low in CO_2 (Y. Li, Xu, Haq, Zhang, & Zhu, 2014). C_4 plants make use of a more efficient enzyme upstream of RuBisCO to fix atmospheric CO_2 in an ATP-dependent manner. This forms malate or aspartate in the mesophyll cells. The malate is transported to isolated bundle sheaths housing RuBisCO, where it is then decarboxylated. Decarboxylation releases the fixed carbon from malate as CO_2, and enriches the concentration surrounding RuBisCO for the creation of sucrose using energy from the light-harvesting reaction. Extensive research has been focused on engineering C_4 mechanisms of photosynthesis into C_3 plants in order to improve the efficiency of photosynthesis in those host plants, such as rice (von Caemmerer, Quick, & Furbank, 2012).

1.5 Carbon Concentrating Mechanisms to Increase Carbon Capture

1.5.1 Algal Bicarbonate Transporters Increase [CO_2] at RuBisCO

Another means of increasing photosynthesis without increasing the efficiency or abundance of the enzyme RuBisCO is to increase the availability of its substrate, CO_2. Although RuBisCO has relatively slow enzymatic activity, phosphoglycerate production

rate has been shown to increase with increasing levels of atmospheric carbon in a controlled environment (Long, Ainsworth, Rogers, & Ort, 2004). Under normal conditions in vascular plants, carbon is freely diffused into the chloroplast through the cellular membranes in the form of atmospheric CO_2. This does not allow for a method to increase the concentration of carbon for RuBisCO because the concentration cannot increase beyond atmospheric levels. However, in some special classes of photosynthetic organisms, including cyanobacteria and algae, mechanisms have evolved to increase the concentration of CO_2 available to RuBisCO through a designated transporter; transporting CO_2 in the form of bicarbonate (HCO_3-) (Badger, Kaplan, & Berry, 1980).

Unlike gaseous atmospheric CO_2, HCO_3- cannot freely diffuse across cellular membranes, so it requires a designated transporter, and can establish a concentration gradient between membranes. Once HCO_3- is transported into the cell, an enzyme called Carbonic Anhydrase catalyzes the reversible reaction of HCO_3- back to CO_2 for fixation by RuBisCO (Moroney et al., 2011). It has been proposed that engineering CO_2 concentrating mechanisms (CCM) from cyanobacteria or aquatic algae into plants could improve the rate of photosynthesis without directly modifying RuBisCO (Price, Badger, & von Caemmerer, 2011).

Figure 1 shows the CCM in the microalgae, *Chlamydomonas reinhardtii* (Y. Wang & Spalding, 2014). The CCM includes several putative bicarbonate transporters, which are proposed to pump HCO_3- across the plasma membrane and chloroplast envelope to increase CO_2 concentrations at RuBisCO under CO_2 limiting conditions (Fig. 1; large red dots). Limiting CO_2 Inducible Protein (LCIA) has been shown to pump bicarbonate across the chloroplast envelope during conditions of very low CO_2 (Y. Wang

& Spalding, 2014) . A second supposed bicarbonate transporter at the chloroplast envelope has been identified, called Chloroplast Carrier Protein 1 (CCP1), but is not yet well characterized. It is presumed that due to the extreme environment in which these organisms live and where CO_2 is in limiting supply, the transporters evolved to ensure survival.

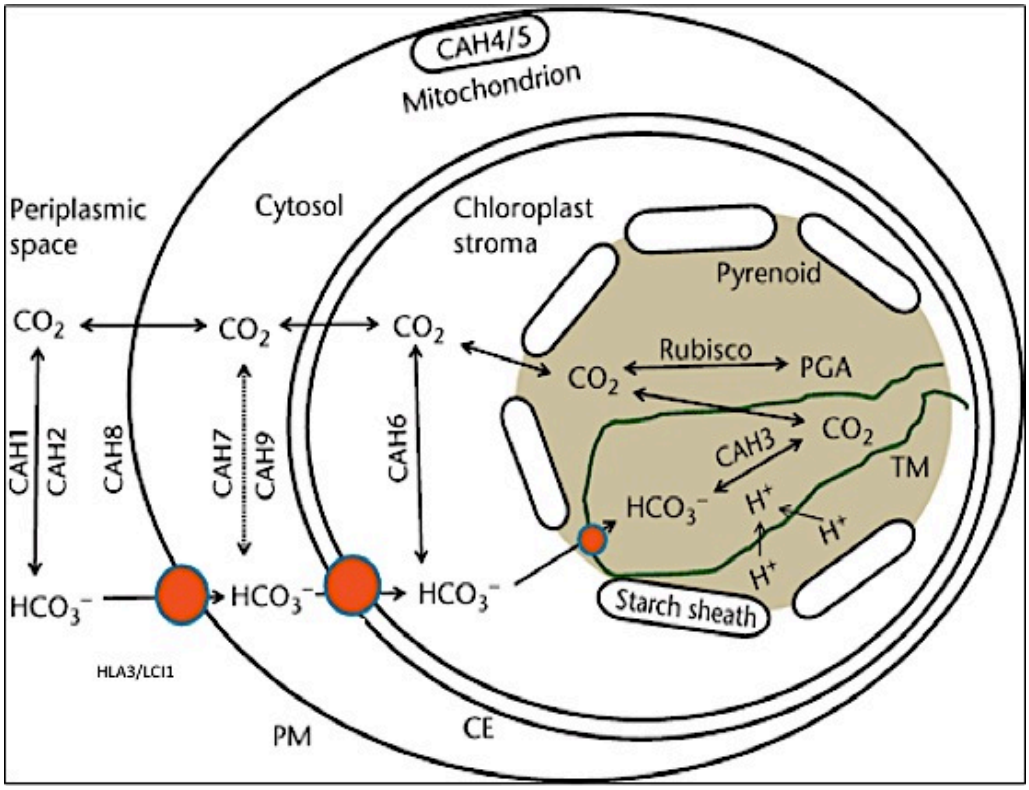

Figure 1: Algal Carbon-Concentrating Mechanism

A model of the algal carbon concentrating mechanism (LCIA/ CCP1) from *Chlamydomonas reinhardtii.* LCIA/CCP1 are indicated by the large reg dot on the chloroplast membrane (Y. Wang & Spalding, 2014).

1.5.2 Engineering Bicarbonate Transporters Into *Camelina Sativa*

Our laboratory has expressed LCIA and CCP1 in *C. sativa* to introduce the bicarbonate transporter component of the algal CCM for the purpose of increasing

photosynthetic capacity. Through improving substrate abundance to RuBisCO, we aimed to see an increase in available seed oil in transgenic *C. sativa*. The transporters are predicted to localize to the membranes of chloroplast. No target peptide was added to the sequence to direct targeting, as an intrinsic chloroplast target peptide is present from *C. reinhardtii*. As shown in the model in Figure 2, the LCIA/CCP1 algal transporters are expected to pump bicarbonate into the chloroplast in cohort with sodium through an established sodium-ion gradient. The bicarbonate is then converted to CO_2 by a Carbonic Anhydrase (CA), and fixed to RuBP by RuBisCO. Due to the increased substrate abundance available to RuBisCO, photosynthesis output increases, with an observable increase of phosphoglycerate available for sucrose production.

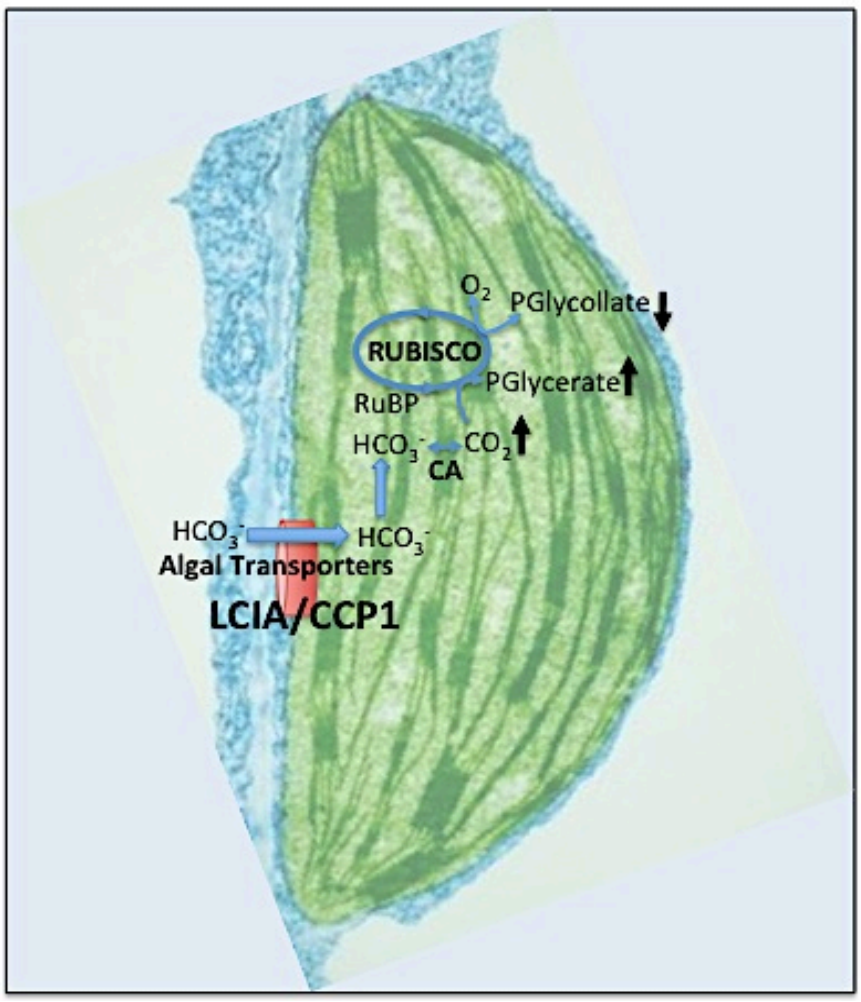

Figure 2: Algal bicarbonate transporters integrated into chloroplast

A model that shows the theoretical insertion of the bicarbonate transporters LCIA/ CCP1 into the chloroplast. Note the pumping of HCO_3- into the chloroplast (Unpublished, Schnell).

Unpublished data from our laboratory shows that homozygous lines of *C. sativa* expressing the CCP1 bicarbonate transporter exhibit an increased CO_2 assimilation rate, as shown in Figure 3. The increase in CO_2 assimilation in the transgenic lines signifies a higher photosynthetic capacity. This is in agreement with our hypothesis that introducing a foreign algal CCM to *C. sativa* will improve photosynthesis through increased substrate availability.

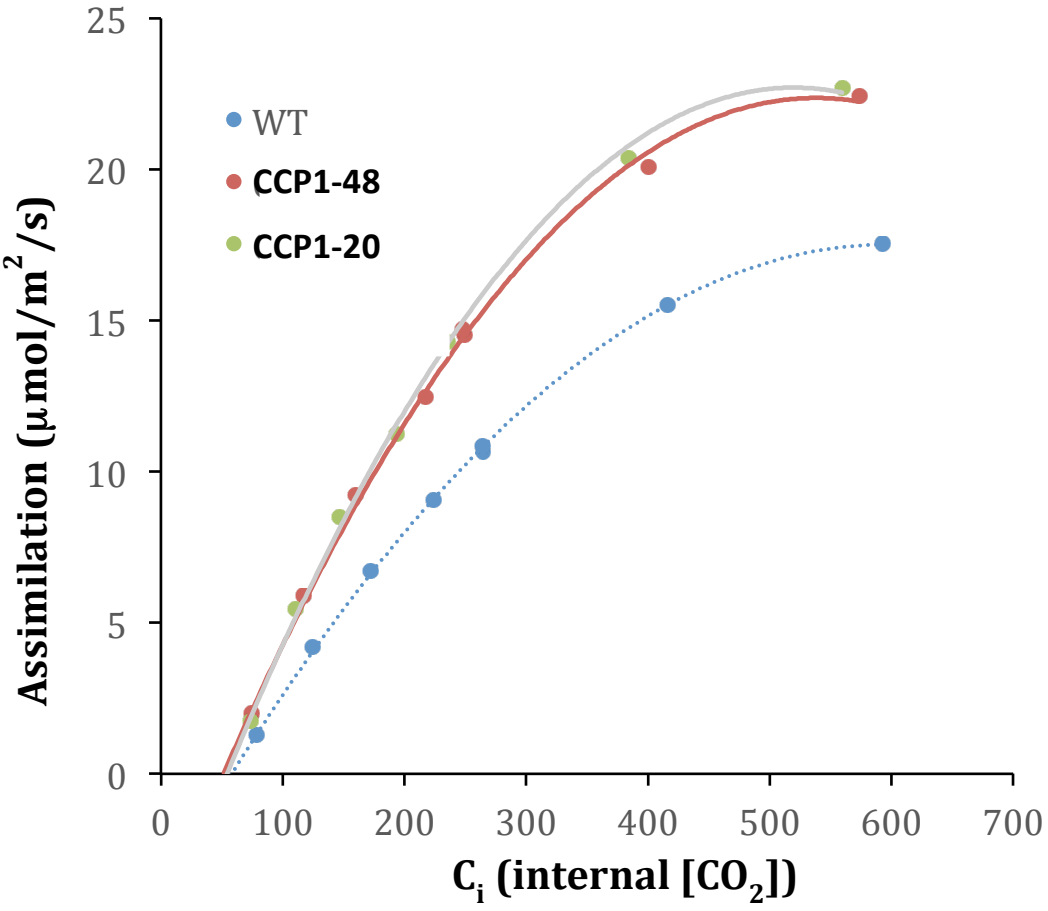

Figure 3: Carbon Assimilation Data

T_3 homozygote lines of CCP1-20 and CCP1-48 exhibit increased carbon assimilation compared to wild type. This difference in assimilation increases as internal CO_2 is increased (Unpublished, Schnell).

Upon doing yield analysis on these transgenic CCP1 *C. sativa*, an increase in overall seed yield, measured by weight, is found in select homozygous lines. This data is shown in Figure 4. From this we conclude that the resulting yield increase is due to the integration of the algal bicarbonate transporter CCP1 through improved photosynthetic efficiency.

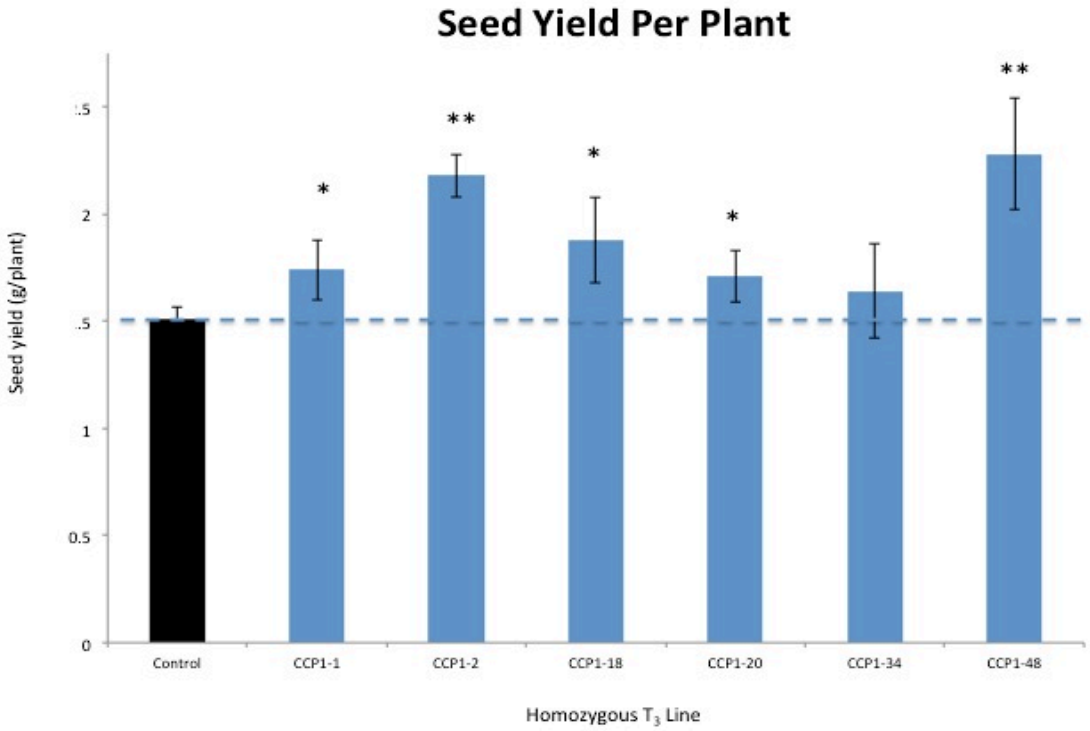

Figure 4: Increased Seed Yield in Transgenic CCP1 C sativa

A graphical representation of seed yield, in grams, of CCP1 *C. sativa* compared to wildtype control. All CCP1 lines tested show an increase in seed yield per plant. Error bars represent standard error of a minimum of three biological replicates (Unpublished, Schnell).

In contrast with our hypothesis, however, transgenic lines showed a decrease in the mass per seed, as shown below in Figure 5. Data from LCIA/CCP1 transgenic lines of *C. sativa* also demonstrate a marked increase in the number of seeds in transgenic plants, but have reduced dry weight compared to naturally occurring *C. sativa*. This is in agreement with phenotypes from expressing CCP1 alone. Although the seeds are smaller in mass, they contain similar oil composition and other physical characteristics. It appears a tradeoff was made: in order to increase seed abundance overall seed weight had to decrease as a result.

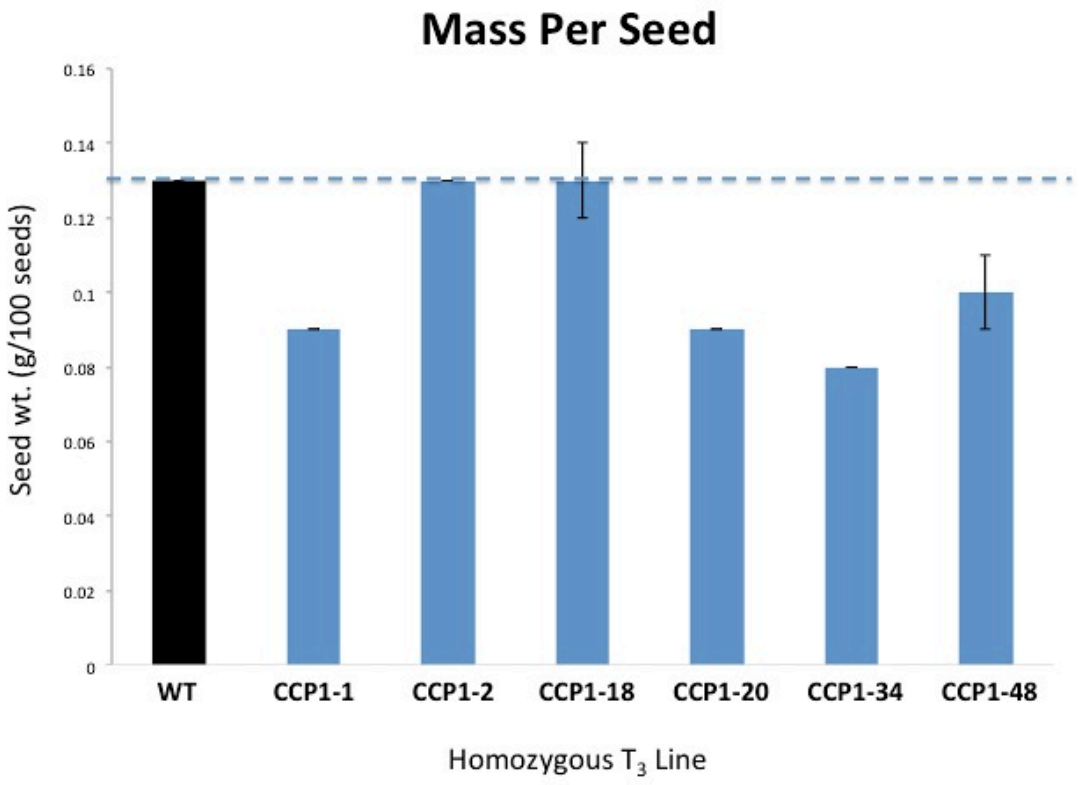

Figure 5 Decreased Mass Per seed in Transgenic CCP1 *C. sativa*

A graphical representation showing decreased seed mass on average in CCP1 transgenic T_3 homozygous lines. Error bars represent standard error of a minimum of three biological replicates (Unpublished, Schnell).

1.6 Adaptation to Elevated Carbon Dioxide

The positive impact on growth and yield observed in C_4 and CAM plants demonstrates that carbon concentrating mechanisms are effective means of increasing carbon assimilation at RuBisCO. Furthermore, the positive impact of increased CO_2 concentrations on photosynthesis have been demonstrated by experiments in which C_3 plants have been grown under high CO_2 concentrations. In these conditions, photosynthesis is shown to increase, with increased growth and productivity. However, it's been shown that C_3 plants adapt to increased CO_2 by reducing photosynthetic

capacity, thereby limiting the overall yield increases below the calculated theoretical gains (Ainsworth & Rogers, 2007; Leakey, Ainsworth et al., 2009; P. Li et al., 2008).

Photosynthetic capacity exhibited a reduction through increased closure of the stomata and a decrease in the amount of RuBisCO in the leaves (Ainsworth & Rogers, 2007; Leakey et al., 2009). RuBisCO is down regulated due to increased catalytic efficiency of CO_2 fixation, due to increased CO_2 in the atmosphere. This allows for a greater concentration gradient between membranes in the chloroplast, enriching the concentration around RuBisCO. The resulting decrease of RuBisCO levels has also been shown to be a result of limitations on the regeneration of RuBP (Ainsworth & Rogers, 2007; Leakey et al., 2009).

The increase in ability to concentrate carbon around RuBisCO causes a change in stomatal closure to balance CO_2 intake with water loss due to transpiration (Ainsworth & Rogers, 2007). Because stomata closure decreases CO_2 flux into the leaves and transpiration of water out of the leaves, plants develop a higher drought tolerance. This is seen in our transgenic CCP1 *C. sativa*, where plants show an increased lifespan in drought conditions, wilting at later stages of drought. CCP1 plants also show better Water Use Efficiency (WUE), retaining a greater water percentage in the growing medium between waterings.

As previously stated, RuBisCO accounts for the majority of soluble protein in leaves. RuBisco is also a storage compartment for nitrogen, with plants allocating approximately one-seventh of total nitrogen to RuBisCO. Therefore, a decrease in the amount of RubisCO due to CO_2 acclimation, results in an increased availability of nitrogen for plant use. Plant Nitrogen Use Efficiency (PNUE) is therefore increased in

plants grown in high CO_2, due to less nitrogen demand of RuBisCO. This can result in positive effects from reallocation of nitrogen, however only in conditions where nitrogen is in limiting supply. For this reasons plants grown in high CO_2 exhibit better growth at lower nitrogen levels compared to controls. This effect is not seen when growing plants in excess nitrogen.

1.7 Respiration and Acclimation to CO_2

Photoassimilate production from photosynthesis exhibits an increase at high CO_2 conditions even though aspects of photosynthesis, such as RuBisCO, are down regulated. The increased photoassimilates are incorporated into cell wall biosynthesis, increasing carbohydrate content. Photoassimilates are destined for transport to "sink" tissues from the "source" leaves, as previously stated. The loading of carbohydrates into the transportation compartment of the plant, the phloem, requires approximately 30% of cellular energy in the leaves, in the form of ATP (Amthor, 2000). The mitochondria are responsible for the energy production that feeds other processes throughout the cell, such as phloem loading. ATP production is controlled through respiration of the mitochondria, where oxygen is used to metabolize carbohydrates into energy.

Using this rationale, it may be expected that increased photoassimilate production could put an energy demand on the cell for increased export of carbohydrates to the phloem (Leakey, Xu et al., 2009). This in turn will result in an increase of cellular respiration at increased CO_2 concentration to meet cellular demand. Transcript profiles of plants grown in increased CO_2, indeed, show an increase in cellular respiration components and a decrease in photosynthetic components (Leakey et al., 2009).

Mitochondria are also found in higher frequency in cells of leaves grown in high CO_2, supporting a greater degree of respiration.

Respiration level has been shown to depend greatly on substrate availability (Williams & Farrar, 1990). Respiration rate increases with increasing availability of carbohydrates. With greater carbohydrate integration into the cell wall, there is a greater availability to the mitochondria to undergo respiration. This removes carbohydrate stores that were destined for sink transportation, negatively affecting carbohydrate partitioning to the seed.

As a rationale for this, and thinking about this in terms of Monteith crop yield relationships, introducing the bicarbonate transporter resulted in an increase in photosynthetic efficiency but a decrease in partitioning efficiency, or harvest index. This may explain the result of increased seed yield of decreased mass per seed, seen in CCP1 expressing *C. sativa*. Increasing partitioning efficiency, therefore, may result in the full yield potential being realized. As a consequence, achieving maximal yield gains will require a combination of increased carbon capture with increased allocation from source to sink tissues.

1.8 Carbon Allocation Limits Yield

1.8.1 RNA Sequencing Analysis of CCP1 *Camelina Sativa*

In order to determine which genes are responsible for the observed results, RNA-sequencing analysis was performed on a sample from a CCP1 transgenic line. A subset of the data is shown in Table 1. The gene IDs shown are of up-regulated genes involved in carbohydrate assimilation, gathered from a larger data set showing genes differentially regulated compared to wild-type *C. sativa*. Of note is gene Csa15g017550, a putative

plant invertase inhibitor, which shows an infinite positive-fold change compared to wild-type. This observation shows that this gene may be up regulated, or turned on, in response to the insertion of the bicarbonate transporters.

Table 2: RNA Sequencing Analysis of CCP1

Gene ID	Note	Fold Change
Csa15g017550	Plant invertase/pectin methylesterase inhibitor	∞
Csa10909s010	Dicarboxylate transport 2.1	∞
Csa19g031010	UDP-glucosyl transferase 71B8	4.60965
Csa13g043350	UDP-Glycosyltransferase superfamily protein	4.13038
Csa01g044640	NADP-malic enzyme 1	2.66152
Csa17g089960	UDP-Glycosyltransferase superfamily protein	2.46725
Csa08g010670	UTP-galactose-1-phosphate uridylyltranferases	2.07423
Csa13g055230	Sugar transporter protein 7	2.00485

1.8.2 Invertases and Carbon Allocation

Plant invertases and their respective inhibitors have been shown to have a significant role in carbohydrate partitioning to seeds. Invertases accomplish this through regulating phloem loading, unloading and sucrose transport. Phenotypic results of overexpression of plant invertase inhibitors has shown a reduced seed weight but increase in seed number, which mimics the observed phenotype of transgenic CCP1 *C. sativa*. This observation supports the RNA-sequencing analysis that a plant invertase inhibitor may be resulting in the observed phenotype of small seeds of increased abundance, even under carbon-concentrating conditions.

Plant invertases have been identified as members of the sucrose trafficking system in vascular plants, as shown in Figure 6. Invertases function to irreversibly cleave the polysaccharide sucrose to its respective monosaccharides: glucose and fructose. These

resulting hexose sugars play an important role in cell signaling and regulation of different processes, such as defense (Lammens et al., 2008).

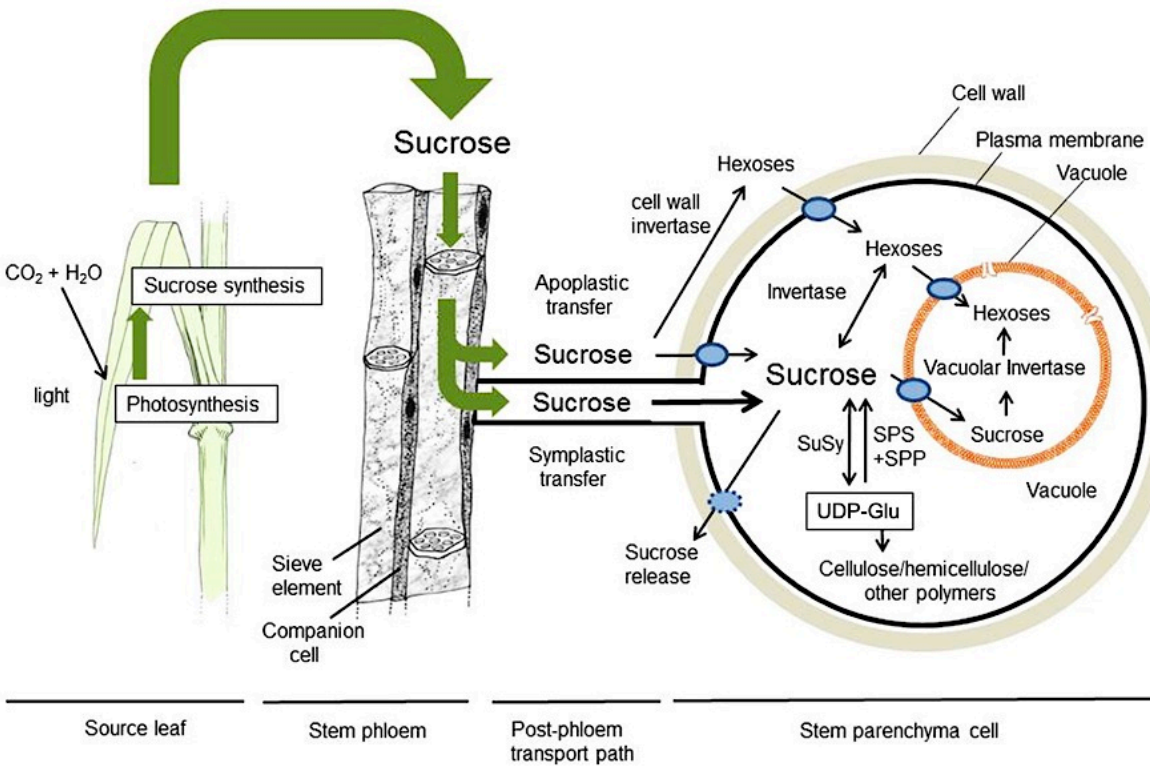

Figure 6: Sucrose transport in sugar cane

Photosynthesis occurs in the source leaf, as indicated, producing sucrose that is loaded into the stem phloem. Sucrose is transported to the sink tissue through symplastic transfer or apoplastic transfer. Apoplastic transfer acts on sucrose that escapes from the phloem. Sucrose is then acted on by invertases for apoplastic transfer (cell wall invertase) (J. Wang, Nayak, Koch, & Ming, 2013).

Different classes of plant invertases include cytoplasmic, vacuolar, and apoplastic (cell wall), all shown in Figure 6. These classes are characterized by their location in the cell. Vacuolar and apoplastic plant invertase are considered acid invertases due to the optimum acidic pH (~4.5-5.0) at which their conformation is stable (Sturm, 1999). This is the pH at which they also most effectively cleave sucrose. Acid invertases are also considered Beta-fructofuranosidases because they attack the disaccharide of the fructose

residue in sucrose. This is in contrast to cytoplasmic invertase, which is considered an alkaline invertase, at optimum basic pH (~7.0-7.8), and shows specificity for sucrose.

Eight acid invertases have been identified in A. thaliana; six cell wall and two vacuolar invertases (Sherson, Alford, Forbes, Wallace, & Smith, 2003). Acid invertases exhibit a high level of stability due to their glycan content. Transcriptional regulation has been exhibited for these invertases by glucose repression (Sturm, 1999). However, the requirement for sharp changes in hexose levels at certain developmental stages, and in defense responses, has implicated posttranscriptional regulation by a proteinaceous inhibitor (Hothorn, D'Angelo, Marquez, Greiner, & Scheffzek, 2004; Rausch & Greiner, 2004).

1.8.3 Cell Wall Invertase Regulates Phloem Transfer of Sucrose to Sink Tissues

Six cell wall invertases have been identified in *A. thaliana*. They show differential expression in different tissues and stages of growth (Sherson et al., 2003). Previous work has shown that tissue-specific constitutive expression of cell wall invertase (CWI) can result in a dramatic increase in carbohydrate allocation to the sink tissues. Results show increases in seed number, seed size, and sugar content in a variety of host organisms such as tobacco, tomato, maize, and rice

Cell wall invertase activity in sink tissues is implicated in phloem unloading of sucrose (Sturm, 1999). Over-expression of apoplastic (cell wall) invertase in potato tubers results in increased tuber size of lesser frequency (Sonnewald et al., 1997). It has also been shown to play a role in early seed development in cotton, triggering the transition of carbohydrates from pre-storage to storage (L. Wang & Ruan, 2012). High invertase activity at the globular-embryo stage and torpedo-embryo stage triggers

allocation of sucrose into developing seed compartments (Bate, Niu, Wang, Reimann, & Helentjaris, 2004; L. Wang & Ruan, 2012).

Invertase activity at source tissues is implicated to have a role in phloem loading, converting stored carbohydrates in the cell wall to the resulting hexoses (Giaquinta, 1977). Source tissue invertase activity is also implicated to have a role in the defense response to factors such as wounding. It is not clear how invertase activity at source leaves stimulates phloem loading. However at alkaline pH, when CWI is inactive, phloem loading is inhibited and carbohydrates remain in source tissue—implicating a role for CWI. The increased hexose concentration at source tissues might trigger sucrose loading into the phloem by interacting with sugar sensing machinery in the cell (Koch, 2004).

1.8.4 Cell Wall Invertase is Regulated Post-Transcriptionally by an Inhibitor

Adjustment of the hexose/sucrose ratio has been shown to act as an important signal that regulates metabolism. As a result CWI activity must be tightly controlled through mechanisms in addition to transcriptional repression. CWI has been demonstrated to show regulation by a proteinaceous inhibitor that outcompetes sucrose for the active site of CWI (Hothorn, Van den Ende, Lammens, Rybin, & Scheffzek, 2010) . This CWI Inhibitor (Cwii) is a small 15-23 kD peptide that interacts with the active site of CWI (Greiner, Krausgrill, & Rausch, 1998; Krausgrill, Sander, Greiner, Weil, & Rausch, 1996). There are four conserved cysteine residues found among Cwiis of different organisms. These cysteine residues are responsible for forming disulfide bonds, which allow the inhibitor to function (Scognamiglio et al., 2003).

Previous work, targeted at silencing the inhibitor of CWI as a means to increase activity of CWI, has been successful. Through induced RNA silencing (RNAi) of the Cwii, CWI activity is shown to increase dramatically, and also produce similar physiological effects as overexpression of CWI, such as increase in seed size and number in tomato (Jin, Ni, & Ruan, 2009). The resulting fruits also contain a higher hexose level.

1.9 Aims

I aim to mirror these works through introducing a construct inducing RNA silencing of Cwii isoforms to transgenic *C. sativa*. These plants are engineered to contain the algal bicarbonate transporters LCIA and CCP1. The purpose for silencing of the Cwii isoforms is to create an increased allocation of carbon to seed sink tissues in an effort to increase ending seed mass. The decrease in the mass per seed that has resulted from the insertion of algal bicarbonate transporters LCIA/CCP1 may be due to decreased activity of cell wall and vacuolar invertases by increased expression of their inhibitors. Therefore, I aim to silence these inhibitors to increase invertase activity at previous points of regulation.

1.10 Hypotheses

I hypothesize that improving light conversion efficiency through improved photosynthesis with LCIA/CCP1 bicarbonate transporters will result in acclimation to increased CO_2 levels within the plant. This will influence gene expression, and drive a decrease to partitioning efficiency of carbohydrates to the seeds. This results in a decrease in dry seed mass. If this is true then it can be hypothesized that increasing the partitioning efficiency through RNA mediated silencing of Cwii could cease photosynthesis acclimation at high CO_2, making calculated theoretical yield potentials

achievable. I hypothesize that introducing Cwii RNAi constructs to *C. sativa* containing the bicarbonate transporters LCIA/CCP1 will result in a synergistic, and marked increase in yield potential, greater than expression of either transgene alone.

CHAPTER 2

2 RESULTS & DISCUSSION

2.1 Identification & Bioinformatic Analysis of Cwii

The cell wall invertase isoforms in *A. thaliana* have exhibited regulation by two cell wall/ vacuolar invertase inhibitor proteins: Cell wall/vacuolar inhibitor of fructosidase 1 (C/VIF1) and Cell wall/ vacuolar inhibitor of fructosidase 2 (C/VIF2). Beta-fructosidase is another common descriptive phrase for acid invertases. Due to *C. sativa*'s close genetic relationship to *A. thaliana*, C/VIF1 (Gene ID: 841214; TAIR ID: AT1G47960) was used to tblastn search the *C. sativa* genome for orthologs. Prairie Gold Genome Prairie resource was used to perform the tblastn searches (http://www.camelinadb.ca/) and found six significant sequence alignments corresponding to inhibitor-like proteins, with a max E-value cutoff score of 10e-10. These genes were indicated by chromosome location: Chr17 (5e-42), Chr3 (3e-41), Chr14 (2e-40), Chr 15 (2e-25), Chr 19 (2e-24), and Chr1 (1e-23). Due to the hexaploidy of C. sativa, where there are three copies of each gene, this was determined to represent two sets of cell wall invertase inhibitor genes in *C. sativa*. The first set, Csa03g051630, Csa14g051860, and Csa17g075360, which was of higher similarity to AT1G47960, was determined to reliably represent the C/VIF 1 ortholog in *C. sativa*. This gene set was designated isoform Cwii1.

C/VIF2 isoform from *A. thaliana* (Gene ID: 836583; TAIR ID: AT5G64620) was used to tblastn search the *C. sativa* genome and found three significantly similar alignments, with a max E-value cutoff score 10e-10. The chromosome positions are:

Chr2 (2e-75), Chr18 (4e-74), and Chr11 (1e-73). This corresponds to a single set of invertase inhibitor genes: Csa02g074170, Csa18g038260, Csa11g101740, and was designated isoform Cwii2.

Once the sequences for Cwii1 and Cwii2 were identified we performed homology modeling and bioinformatics to find sequence similarities in other organisms. The identified Cwii1 and Cwii2 nucleotide sequences were translated using ExPASy (Expert Protein Analysis System) translation software on the SIB ExPASy Research Portal page (Artimo et al., 2012). An NCBI BLAST search of the protein FASTA sequence (blastp) was conducted (Altschul et al., 2005; Altschul et al., 1997). Cwii1 shows greatest similarity with *A. thaliana* C/VIF 1 (ref: NP_564516.2), with 88% similarity. This gives an E-value of 3e-83 and a max score of 255. Similarly, Cwii2 shows greatest similarity with *A. thaliana* C/VIF 2 (ref: NP_201267), with 88% similarity. The E-value is 5e-109 and a max score of 321. The protein sequences were more distantly similar to those from tomato, potato, and tobacco.

The sequences showing similarity with either Cwii1 or Cwii2 were obtained in order to perform a more direct comparison between sequences through sequence alignment using Clustal Omega (Goujon et al., 2010; Larkin et al., 2007). A phylogenetic relationship between sequences was created and is shown in Figure 7. As predicted, *C. sativa* Cwii isoforms 1 and 2 cluster most closely with those from *A. thaliana* (TAIR IDs: AT1G47960 and AT5g64620), emerging from a common ancestor. Cwii 2 from *C. sativa* shows a more distant relationship to those from tomato (AGC75063 and CAA09420), and potato (AFI47461), as indicated by their separate clades. However, Cwii 2 does cluster near tobacco (Y12805), possibly implicating more of a role in leaf tissue. Those

of potato and tomato cluster in the same clade, and branch closely from those of Cwii 1 in *C. sativa,* this might indicate more of a sink role for Cwii 1 such as in vacuoles of differentiating tissues.

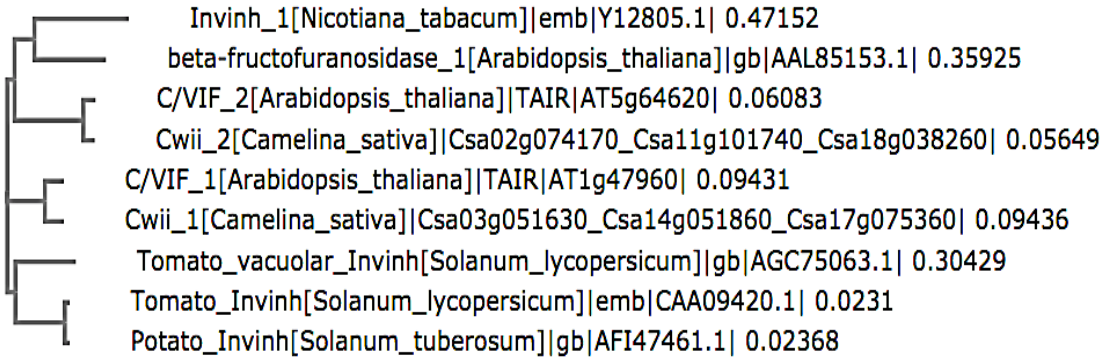

Figure 7: Phylogeny of Cwii1 and Cwii2

Phylogenetic analysis of Cwii isoform contigs from tomato (*Solanum lycopersicum)*, tobacco (*Nicotiana tabacum),* potato (*Solanum tuberosum)*, *Arabidobsis thaliana,* and *Camelina sativa*. Gene bank accession numbers are indicated. Phylogenetic tree was created using Clustal Omega.

The Arabidopsis gene-imaging tool (Arabidopsis eFP Browser), available online at the Bio-Analytic Resource for Plant Biology at the University of Toronto, allows for the visualization of expression data in *A. thaliana* (Winter et al., 2007). The Arabidopsis eFP Browser works by searching for the TAIR (**T**he **A**rabidopsis **I**nformation **R**esource) gene id and generating an image showing expression in different tissues. The TAIR gene id is an id defining locus location, and can be found using the TAIR database (Huala et al., 2001). The TAIR ids for Cwii1 and Cwii2 are AT1g47960 and AT5g64620, respectively, as previously indicated. The Cwii1 ortholog in *A. thaliana*, C/VIF1 is predicted to show expression at higher levels in developing pollen and seed tissue. This is shown in Figure 8 with areas of red color indicating higher absolute levels of expression in said tissue. The Cwii2 ortholog in *A. thaliana*, C/VIF2 is predicted to show expression

at greater levels in green-leaf tissue and senescing leaves, as shown in Figure 9. Cwii2 is also more expressed in seed embryos at the torpedo to walking stick stages of seed development.

A collaborator group, the Sederoff Laboratory, from North Carolina State University, looked at the expression of the Cwii1 and Cwii2 orthologs in C. sativa. Primers were designed for the *C. sativa* ortholog Cwiis, isoforms 1 and 2, and RNA expression analysis by quantitative reverse transcriptase-PCR (qRT-PCR) was performed on both mature seed and young leaf tissue. Cwii1 and Cwii2 were found to be expressed at detectable levels in both leaf and seed tissue. Echoing the predicted results in *A. thaliana*, Cwii1 was expressed more in mature seeds, and Cwii2 expressed more in young leaves (Grunden, Michele, Sederoff, & Ada, 2014).

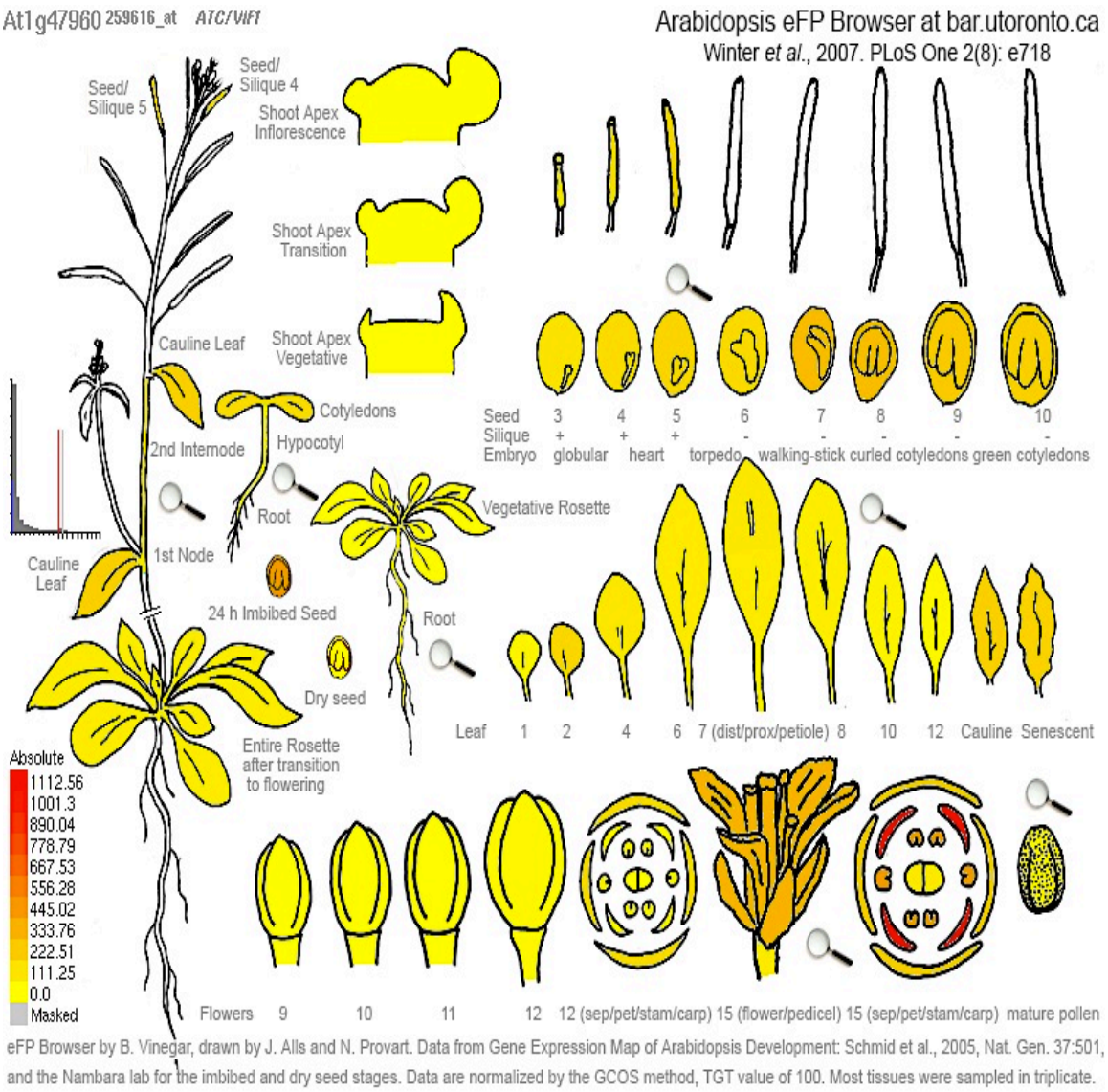

Figure 8: *Arabidopsis thaliana* Expression of Cwii1

Expression profiling of Cwii1 in *A. thaliana* is shown by tissue type. Higher absolute values are expressed as a deeper shade of red, as shown in the figure legend on the left. Cwii1 is expressed more in developing floral tissue (Winter et al., 2007)**.**

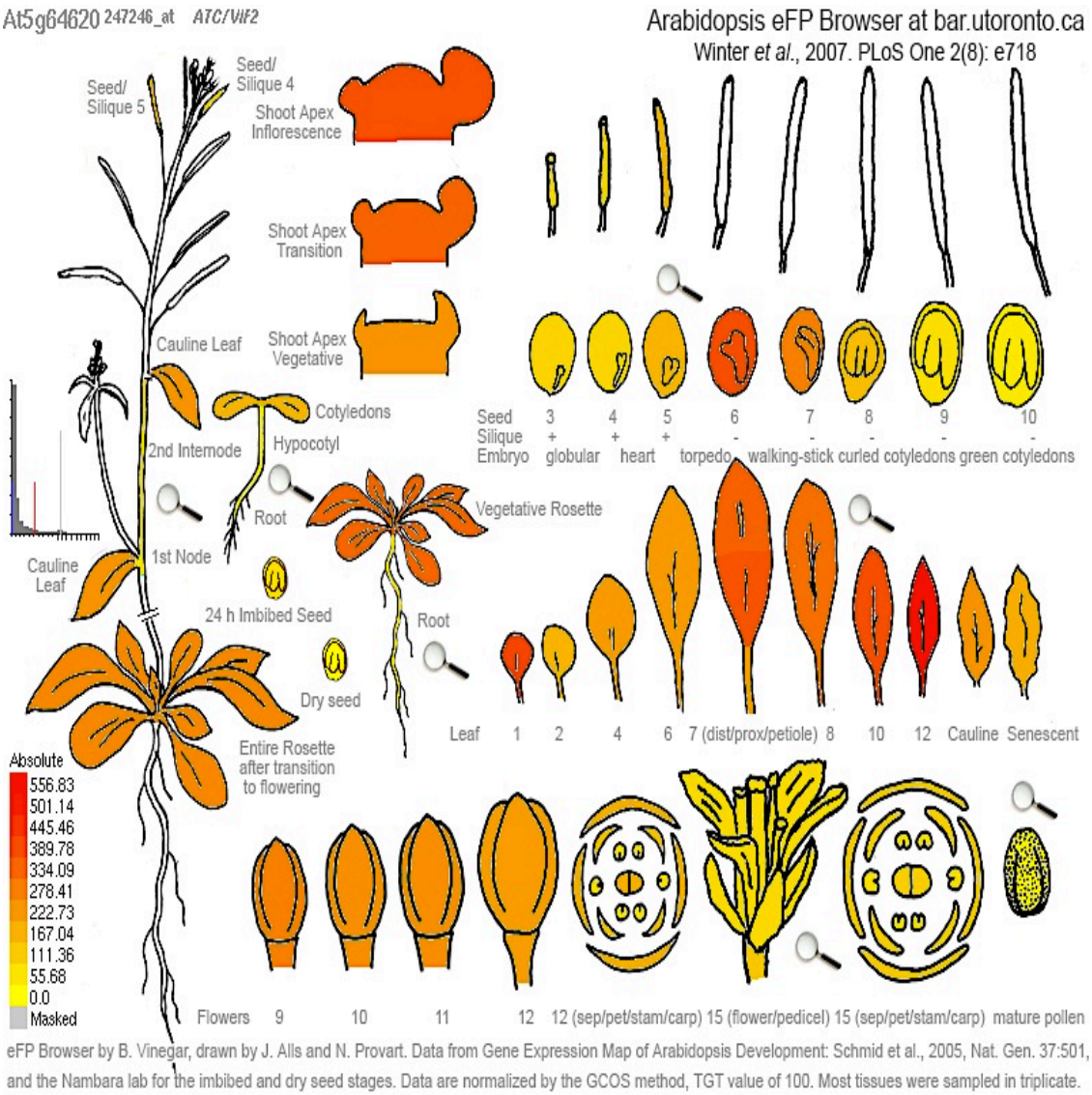

Figure 9 *Arabidopsis thaliana* Expression of Cwii 2

Expression profiling of Cwii2 in *A. thaliana* is shown by tissue type. Higher absolute values are expressed as a deeper shade of red, as shown in the figure legend on the left. Cwii2 is expressed more in mature green-leaf tissue and senescing leaves. Cwii2 also shows higher expression in developing seed embryos at the torpedo to walking stick stages (Winter et al., 2007)**.**

2.2 RNA-mediated Silencing of Cwii1 and Cwii2

We collaborated with the Sederoff group at North Carolina State University to produce the Cwii RNAi constructs that were introduced to *C. sativa* (Grunden et al.,

2014). The constructs were designed to inhibit the two proteinaceous inhibitors of CWI, designated Cwii1 and Cwii2, through RNA-meditated silencing. The process of generating RNAi is well practiced and uses antisense intron specific repression. Cwii1 and Cwii2 were identified through BLAST searches of the sequences of characterized Cwiis from *Arabidopsis thaliana*, *Arabidopsis lyrata*, tomato, and tobacco against the *C. sativa* genome. The sequences of the Cwiis from *A. thaliana* produced two hits of 80% similarity with the sequences that are known as Cwii1 and Cwii2. The E-value cutoff was 10e-10. After confirmation the genes were probed using TAIL-PCR and the native promoters were sequenced (Grunden et al., 2014).

Antisense repression of genes through RNAi mediated silencing is now a well understood practice that is often practiced in laboratories for gene regulation. Complementary base pairs of Cwii1 and Cwii2 were generated to form the antisense portion of the RNAi construct. This forms the silencing hairpin responsible for repression of Cwii mRNA translation. The sense and antisense Cwii sequences were inserted into an expression cassette: pEarlyGate301 was used to house the RNAi construct sequence. pEarlyGate301 contains the resistance genes for bacterial-antibiotic selection on kanamycin, and for plant-herbicidal selection with BASTA. The four constructs (P1S1, P1S3, P2S2, and P2S3) are shown in Figures 11, 12, 13, and 14, respectively. P1S1 contains the promoter for Cwii1 and the sense and anti-sense sequences for the three Cwii1 *C. sativa* genes (Csa03g051630, Csa17g075360, Csa14g051860), shown in Figure 11. P2S2 contains the promoter for Cwii2 and the sense and anti-sense sequences for the three Cwii2 *C. sativa* genes (Csa02g074170, Csa18g038260, Csa11g101740), shown in Figure 13. P1S3 and P2S3 contain both Cwii1 and Cwii2 *C. sativa* genes (Csa03g051630,

Csa17g075360, Csa14g051860, Csa02g074170, Csa18g038260, Csa11g101740) under the control of either the Cwii1 promoter, as in P1S3 shown in Figure 12, or the Cwii2 promoter, as in P2S3 shown in Figure 14.

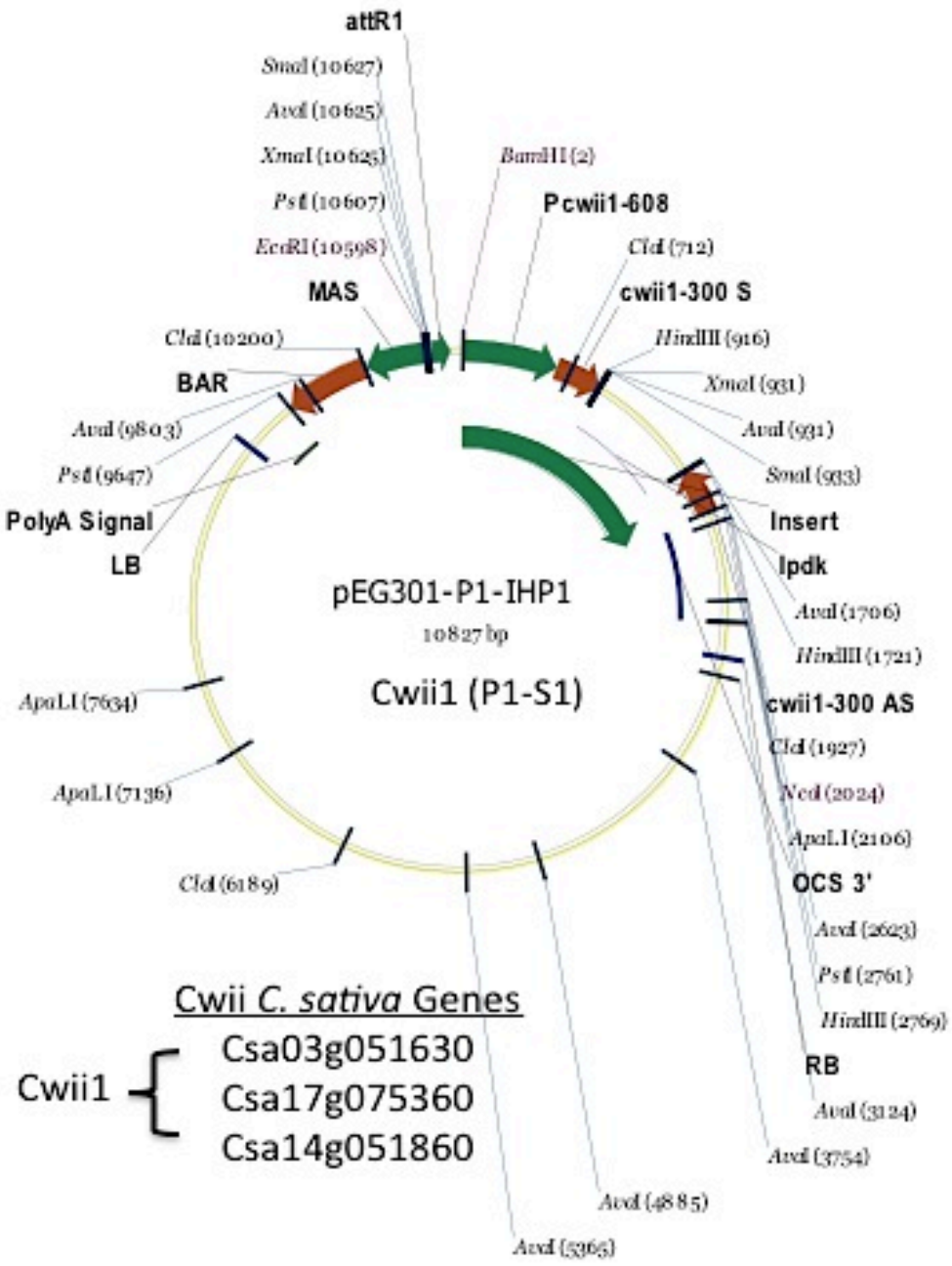

Figure 10: Plasmid Map of P1S1

P1S1 plasmid contains the cwii1 sense (cwii1-300 S) and cwii1 antisense (cwii1-300 AS) for RNAi of cwii1. Cwii1 is under the control of its' native promoter (Pcwii1-608). Basta-resistance gene (BAR) is shown. Specific restriction digest sites (BamHI and Nco1) are highlighted in red.

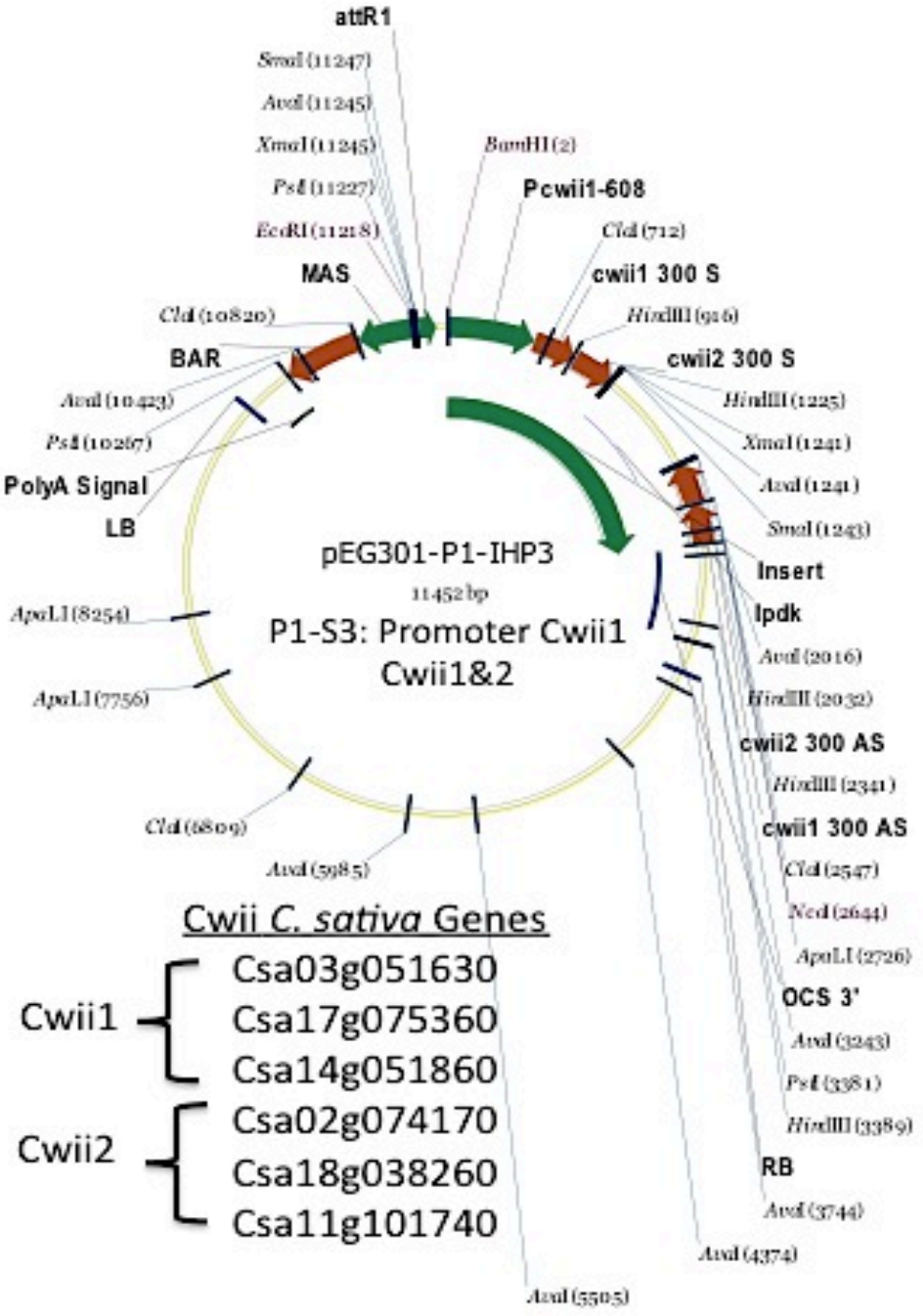

Figure 11: Plasmid Map of P1S3

P1S3 plasmid contains the cwii1 sense (cwii1-300 S) and cwii1 antisense (cwii1-300 AS) for RNAi of cwii1. It also contains the cwii2 sense (cwii2-300 S) and cwii2 antisense (cwii2-300 AS) for RNAi of cwii2. Cwii1 and Cwii2 are under the control of the native Cwii1 promoter (Pcwii1-608). Basta-resistance gene (BAR) is shown. Specific restriction digest sites (BamHI and Nco1) are highlighted in red.

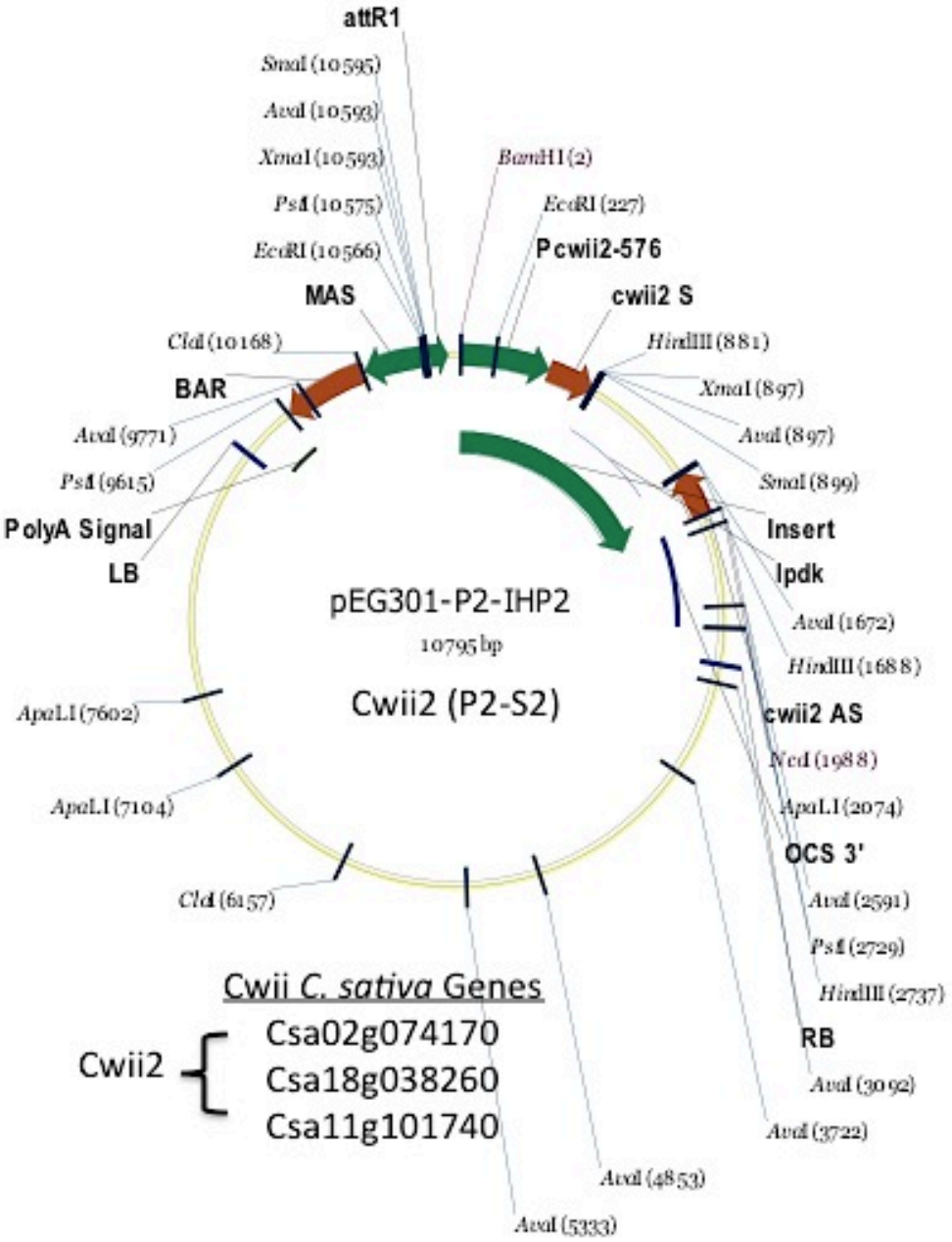

Figure 12: Plasmid Map of P2S2

P2S2 plasmid contains the cwii2 sense (cwii2 S) and cwii2 antisense (cwii2 AS) for RNAi of cwii2. Cwii2 is under the control of its' native promoter (Pcwii2-576). Basta-resistance gene (BAR) is shown. Specific restriction digest sites (BamHI and Nco1) are highlighted in red.

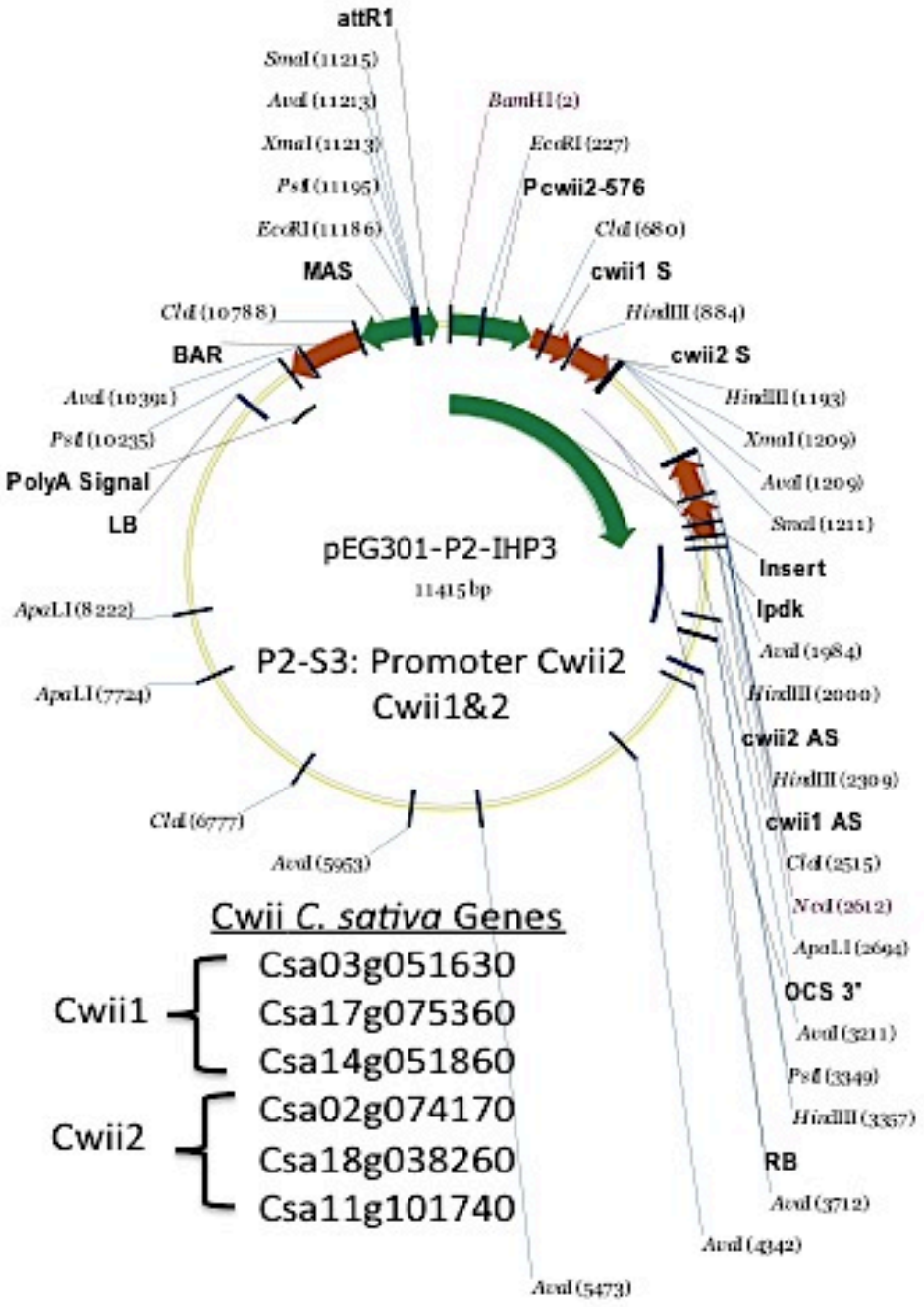

Figure 13: Plasmid Map of P2S3

P1S3 plasmid contains the Cwii1 sense (cwii1 S) and cwii1 antisense (cwii1 AS) for RNAi of Cwii1. It also contains the Cwii2 sense (cwii2 S) and Cwii2 antisense (cwii2 AS) for RNAi of Cwii2. Cwii1 and Cwii2 are under the control of the native Cwii2 promoter (Pcwii2-576). Basta-resistance gene (BAR) is shown. Specific restriction digest sites (BamHI and Nco1) are highlighted in red.

2.3 Transformation into Bacteria and *C. sativa*

The constructs were transformed into *Escherichia coli* (DH5α) and *Agrobacterium tumefaciens* (GV3101) using the heat shock method. Positive transformants were selected using kanamycin. Plasmid prep was performed on resistant colonies, and a restriction digest with BamHI and NcoI was used to confirm construct insertion. The expected band sizes for P1S1 (P1-IHP1) are 2022 bp and 8805 bp, for P2S2 (P2-IHP2) are 1982 bp and 8813 bp, for P1S3 (P1-IHP3) are 2642 and 8810 bp, and for P2S3 (P2-IHP3) are 2610 bp and 8805 bp. The agarose gel image of the restriction digest is shown in Figure 14. The image confirms the presence of each of the four RNAi constructs in replicate.

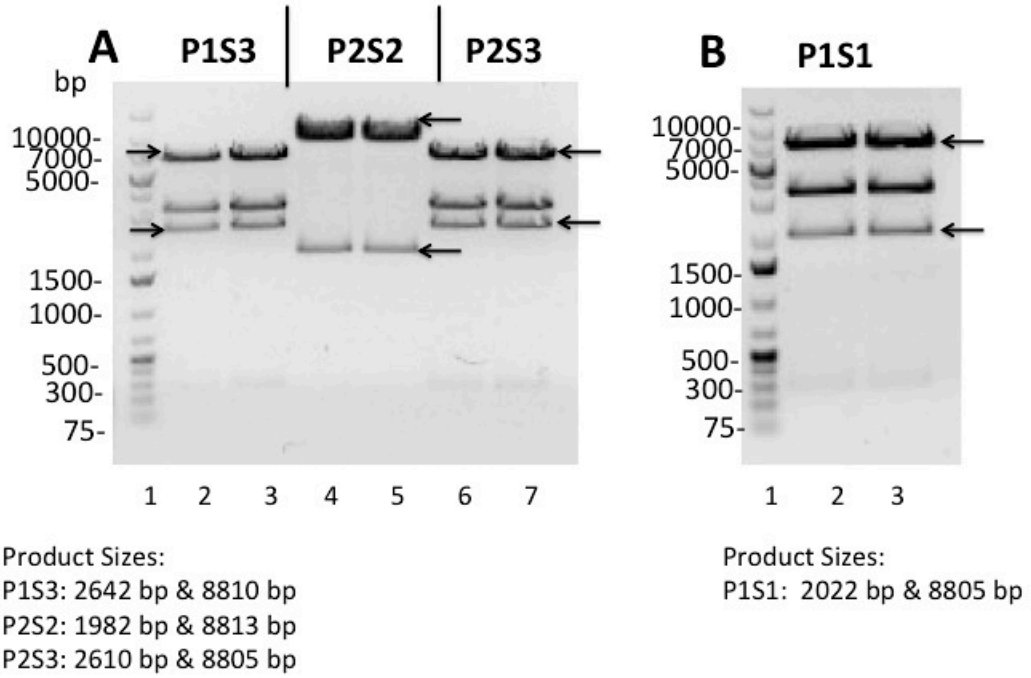

Figure 14: Restriction Digest Confirmation of RNAi Construct Transformation

A 1% Agarose gel image of DNA fragments after digestion with BamHI and NcoI. Panel A, lanes 2 and 3, show digested products of P1S3. Expected product sizes are 2642 bp and 8810 bp. Lanes 4 and 5 show products of P2S2. Expected product sizes are 1982 bp and 8813 bp Lanes 6 and 7 show products of P2S3. Expected product sizes are 2610 bp and 8805 bp. Panel B, lanes 2 and 3, show the digested products of P1S1. Expected sizes are 2022 bp and 8805 bp.

Large cultures of *A. tumefaciens* (GV3101) were grown for plant transformation into *C. sativa* using the floral dip procedure (Lu & Kang, 2008) Transgenic *C. sativa* with the bicarbonate transporters LCIA and CCP1 were transformed with each of the constructs. Line numbers 27 and 34 of the LCIA/CCP1 *C. sativa* were chosen based on unpublished data suggesting improved performance. LCIA/CCP1 homozygous T_3 lines also have complimentary selection markers with the Cwii RNAi constructs, with parental LCIA/CCP1 plants having dsRed selection and the RNAi constructs having BASTA-resistance (bar^r). This makes it possible to screen for successful transformants while tracking both transgenes.

2.4 Confirmation Using Herbicidal Selection and PCR

T_1 Transformants were selected by herbicidal selection of the T_0 progeny using BASTA. Resistant T_1s were transplanted and allowed to reach maturity for collection of T_2 seed. The numbers of T_1s generated for each construct are shown in Table 2.

Table 3: Total number of T_1 Cwii lines

Construct	LCIA/CCP1 27	LCIA/CCP1 34	WT	TOTAL
P1S1	3	6	10	19
P2S2	7	5	12	24
P1S3	14	9	14	37
P2S3	3	13	15	31

DNA was extracted from leaf tissue of the resistant T_1s and Cwii RNAi construct transformation was confirmed via PCR with construct-specific primers, as shown in Table 3. For detection of the Cwii1 RNAi construct the forward primer amplified from the beginning of the Cwii1 target sequence and the reverse primer amplified from the middle of the pdk linker intron. Similarly, for detection of the Cwii2 RNAi construct primers were designed to amplify from the start of the Cwii2 target sequence to midway through the pdk intron linker.

Table 4: Genomic PCR Primers

Construct	Primer Name	Sequence (5'-3')	Annealing Temp (°C)	Product Size (bp)
Cwii1 in: P1S1 P1S3 P2S3	cwii1 trgt-pdk Fwd	ATCTCTAAAGGAGTCCCTAAATTCG	52.8	P1S1: 535
	cwii1 trgt-pdk Rev	AAGCAGATTTCTAACAAAA	52.8	P1S3 & P2S3: 838
Cwii2 in: P1S3 P2S2 P2S3	cwii2 trgt-pdk Fwd	CGTCCTTAAAAAGGTGTTACAAGATT	61.7	P1S3, P2S2, P2S3: 417
	cwii2 trgt-pdk Rev	TGATATTTAATTCATCAAACCAGCTA	61.7	

PCR conditions were optimized for annealing temperature using gradient PCR. Temperatures ranging from 47.9°C to 53.8°C were amplified successfully for Cwii1. 52.8°C was chosen for annealing temperature using these primers in the future. Temperatures ranging from 60.4°C to 61.8°C were amplified successfully for Cwii2. 61.7°C was chosen for annealing temperature using this primer set in the future.

DNA was extracted from BASTA-resistant T_1 plants and probed using appropriate primers for the Cwii gene present in the RNAi construct introduced to the plant. Figure 15 shows confirmation of Cwii1 in both P1S3 and P1S1 BASTA-resistant T_1 plants, with observable products of ~838 bp and ~535 bp, respectively. Figure 16

shows further confirmation of Cwii1 in P1S3. Figure 17 shows confirmation of Cwii2 in P2S2 T_2 plants, with an observable product of ~417 bp. Through PCR detection, RNAi construct insertion was tested to a further degree than BASTA-sensitivity screening alone.

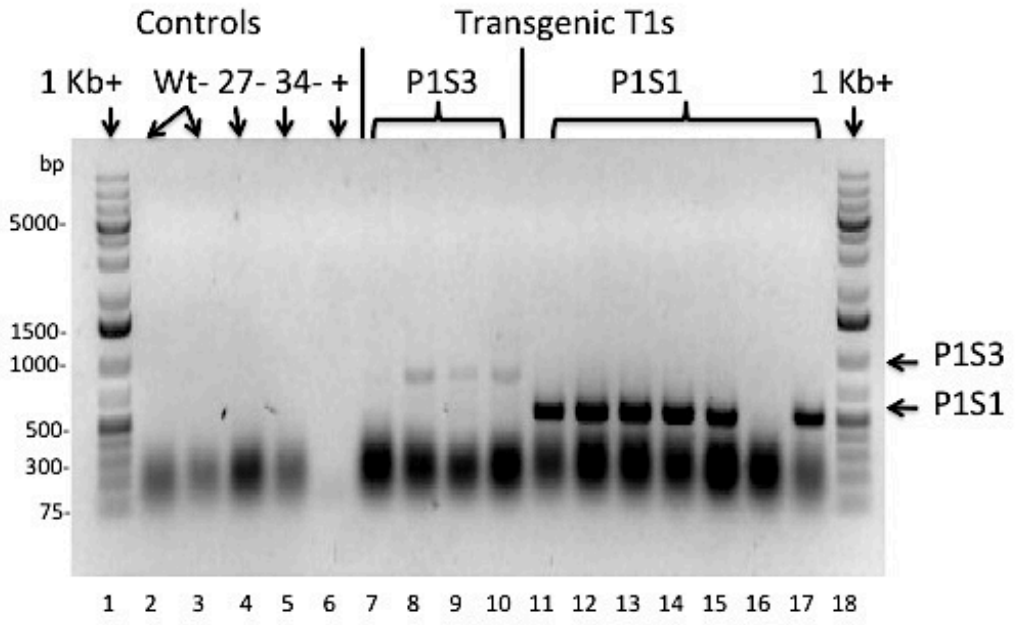

Figure 15 Cwii1 confirmation in P1S3 and P1S1 T_1 Lines

1% Agarose gel stained with SYBR Safe, showing amplified PCR products for genomic T_1 P1S3 and P1S1 DNA. Primers amplifying from Cwii1 to the pdk intron were used. The expected amplified product size is 838 bp for P1S3 and 535 bp for P1S1. 1 Kb-plus DNA ladder is in lanes 1 and 18, and sizes are noted to the left. Wild-type negative controls are in lanes 1 and 2, followed by the LCIA/CCP1 #27 and #34 negative controls in lanes 3 and 4. P1S3 pure plasmid positive control is in lane 6, but shows no amplified PCR product. P2S2 transgenic T_1s are in lanes 5 to 20. The P1S3 and P1S1 amplified fragments are indicated with an arrow.

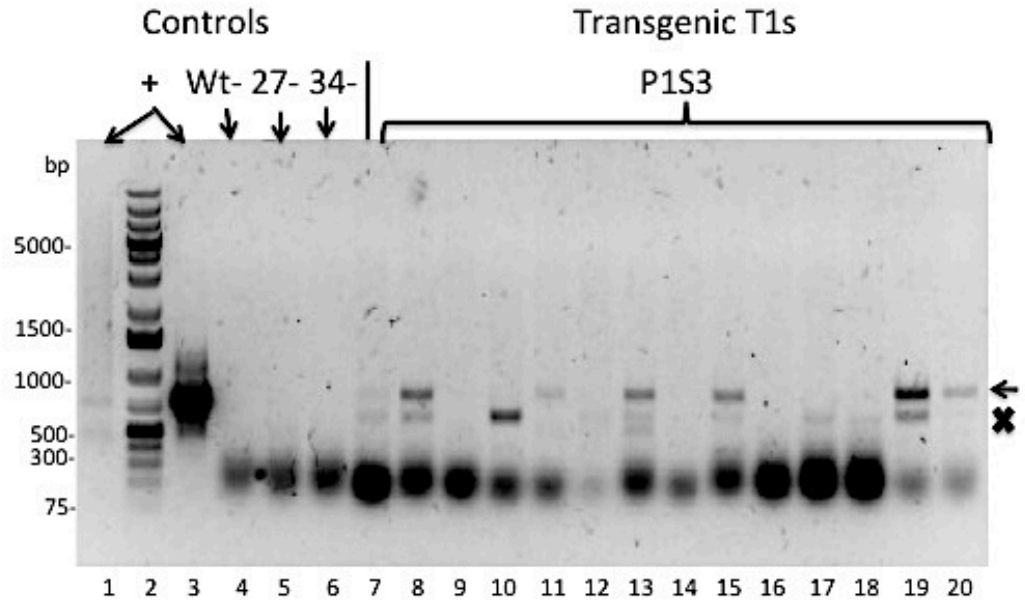

Figure 16: Cwii1 confirmation in P1S3 T_1 Lines

1% Agarose gel stained with SYBR Safe, showing amplified PCR products for genomic T_1 P1S3 DNA. Primers amplifying from Cwii1 to the pdk intron were used. The expected amplified product size is 838 bp. 1 Kb-plus DNA ladder was used and is in lane 2. The sizes are shown to the left of the gel. P1S3 pure plasmid positive control is in lanes 1 and 3. Lane 1 plasmid is diluted five times. The positive control shows correct amplification, but a secondary band is present from nonspecific amplification of Cwii2. The P2S2 amplified fragment is indicated with an arrow to the right, the nonspecific band is labeled with an "x". Wild-type negative control is in lane 4, followed by the LCIA/CCP1 #27 and #34 negative controls in lanes 5 and 6. P2S2 transgenic T_1s are in lanes 5 to 20.

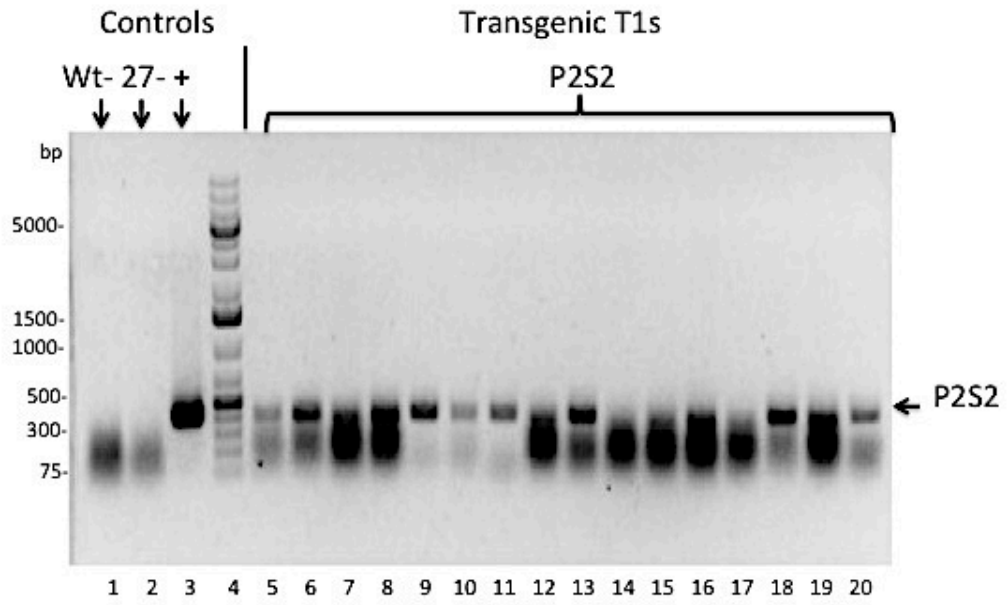

Figure 17: Cwii2 Genomic PCR Confirmation in P2S2 T_1 Lines

A 1% Agarose gel stained with SYBR Safe, showing amplified PCR products for genomic T_1 P2S2 DNA. The expected amplified product size is 417 bp. Wild-type negative control is in lane 1, followed by the LCIA/CCP1 #27 negative control in lane 2. P2S2 pure plasmid positive control is in lane 3 and shows correct amplification. P2S2 transgenic T_1s are in lanes 5 to 20. The P2S2 amplified fragment is indicated with an arrow.

2.5 T_2 Segregation Analysis

T_2 seeds were collected and screened with BASTA for segregation analysis. The genome of *C. sativa* is a hexaploid, meaning there are three copies of each gene; this can be problematic when doing infection by *A. tumefaciens*, as TDNA can be inserted in multiple places in the genome, rendering genetics difficult (Kagale et al., 2014). A set of then currently available T_2 seeds were planted in 72-well trays and screened with BASTA as previously performed. This screening ensures that lines with proper gene insertion are pursued, as these lines will show expected segregation ratios. T_2 plants should show a 1:2:1 segregation of the Cwii RNAi construct, due to the expected heterozygosity of the T_1s. Due to the construct also containing the BASTA resistance gene, 25% of the T_2s

should become BASTA sensitive. The numbers of resistant and susceptible plants were noted as shown in Table 4. Based on this data we selected lines to continue with the T_2 plant generation. Selected lines are indicated also in Table 3.

Table 5: Segregation Analysis of Select T_2 Lines

Construct	T_1 Line	Germinated	bar^s	bar^s: bar^r	Selected for T_2
P1S1	27 1	17	4	24%	YES
	WT 1	16	2	13%	YES
P2S2	WT 1	18	2	11%	YES
	WT 2	17	6	35%	YES
	WT 3	16	2	13%	YES
	WT 4	17	0	0%	NO
	27 1	17	7	41%	YES
	27 2	17	4	24%	YES
	27 3	17	1	6%	NO
	27 4	18	4	22%	YES
	34 1	18	4	22%	YES
	34 2	18	4	22%	YES
P1S3	WT 1	15	4	27%	YES
	27 1	16	4	25%	YES
	34 1	18	2	11%	YES

2.6 Expression of Cwii1 and Cwii2

2.6.1 Primer Design

Primers were designed for the *C. sativa* Cwii isoforms 1 and 2 as shown in Table 5. These primers were to be used for qRT-PCR analysis of the mRNA levels in the generated plants. Primers were optimized for correct annealing temperature for use in the qRT-PCR reaction. Primer optimization was accomplished using a gradient PCR including the DyNAmo HS SYBR Green MasterMix to match qRT-PCR conditions. Optimized temperatures for each primer set are also shown in Table 5. Figure 18 shows the PCR product after gel electrophoresis, and confirms primer specificity and amplification of expected nucleotide sequences.

Table 6: Gene-specific Primers for qRT-PCR

Gene	Primer Name	Sequence (5'-3')	Annealing Temp (°C)	PCR Product Size (bp)
Cwii1	NCsuCWII-1trgt-F	GAAGCTGATCGTGATGGTGA	50.5	398
	NCsuCWII-1trgt-R	TCCCTTGAAACCCTTCTTCA	50.5	
Cwii2	NCsuCWII-2trgt-F	TTCTGTGTCTCGGCTCTCAA	50.5	349
	NCsuCWII-2trgt-R	GACGAATCTCCACCGGATAA	50.5	

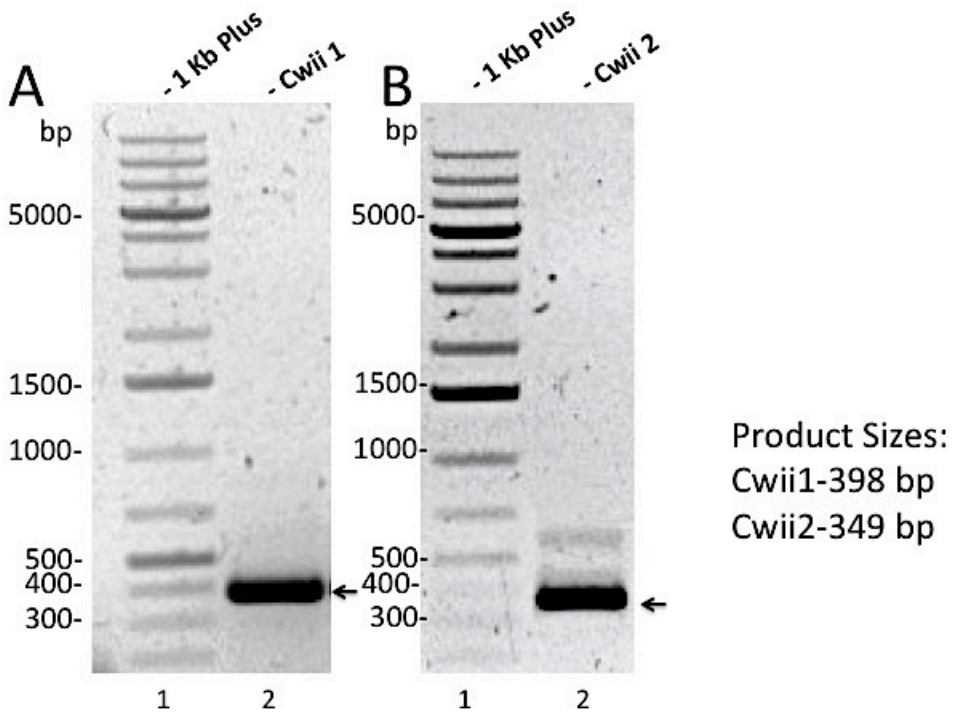

Figure 18: PCR Amplification of Cwii1 and Cwii2 Targets

Image of PCR products of Cwii1 and Cwii2 target sequence amplified with gene-specific primers for Cwii1 and Cwii2. Products were run on a 1% Agarose gel stained with SYBR safe. Panel A, lane 2, shows the Cwii1 pcr product from cDNA, indicated with an arrow. The expected size is 398 bp and is confirmed after comparing to 1 Kb-plus DNA marker shown in lane 1. Panel B, lane 2, shows the Cwii2 pcr product from cDNA, indicated with an arrow. The expected size is 349 bp and is confirmed after comparison with 1 Kb-plus in lane 1. Sizes are noted in base pairs to the left of each panel.

2.6.2 Expression Analysis of Cwii RNAi Transgenics

qRT-PCR was carried out using an Eppendorf RealPlex program and cycler. The *actin* 2 gene was used as a control for a house-keeping gene to compare levels of expression with. Image J software was used to calculate peak intensities from the images taken after running the qRT-PCR products by gel electrophoresis. Peak intensities of experimental samples were normalized to *actin*2 by creating a ratio of Cwii: *actin*2 peak intensity. This represents the level of expression of Cwii relative to *actin*2. Comparing this value to the value of the parental control shows the expression relationship between

samples. The expression levels of Cwii1 and Cwii2 are shown in Figures 19 and 20, respectively. Expression is relative to the parental control, where a value of 1 means equal expression between transgenic and control.

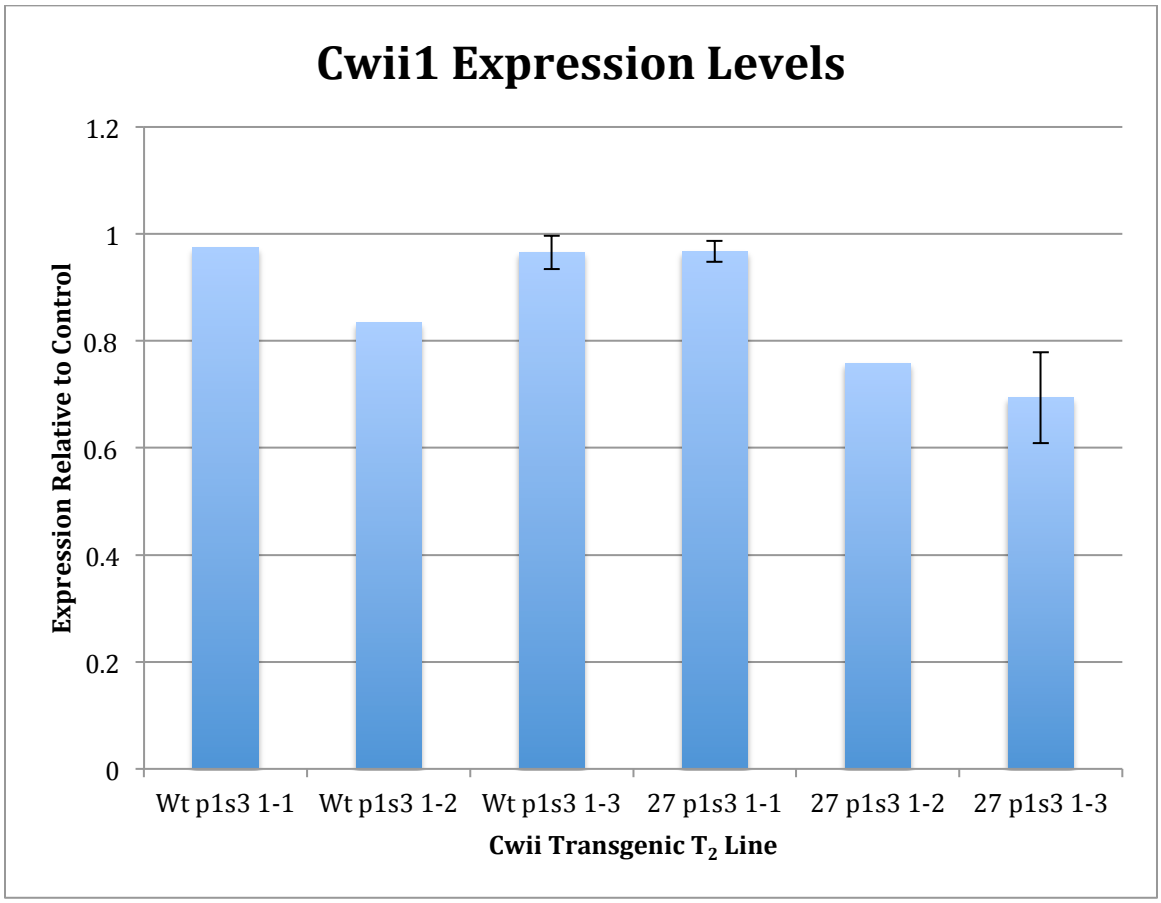

Figure 19: Expression Analysis of Cwii1 in Select T_2 Lines

A graphical representation of Cwii1 expression analysis from select P1S3 T_2 lines. Error bars represent standard error calculated from a minimum of triplicate reactions.

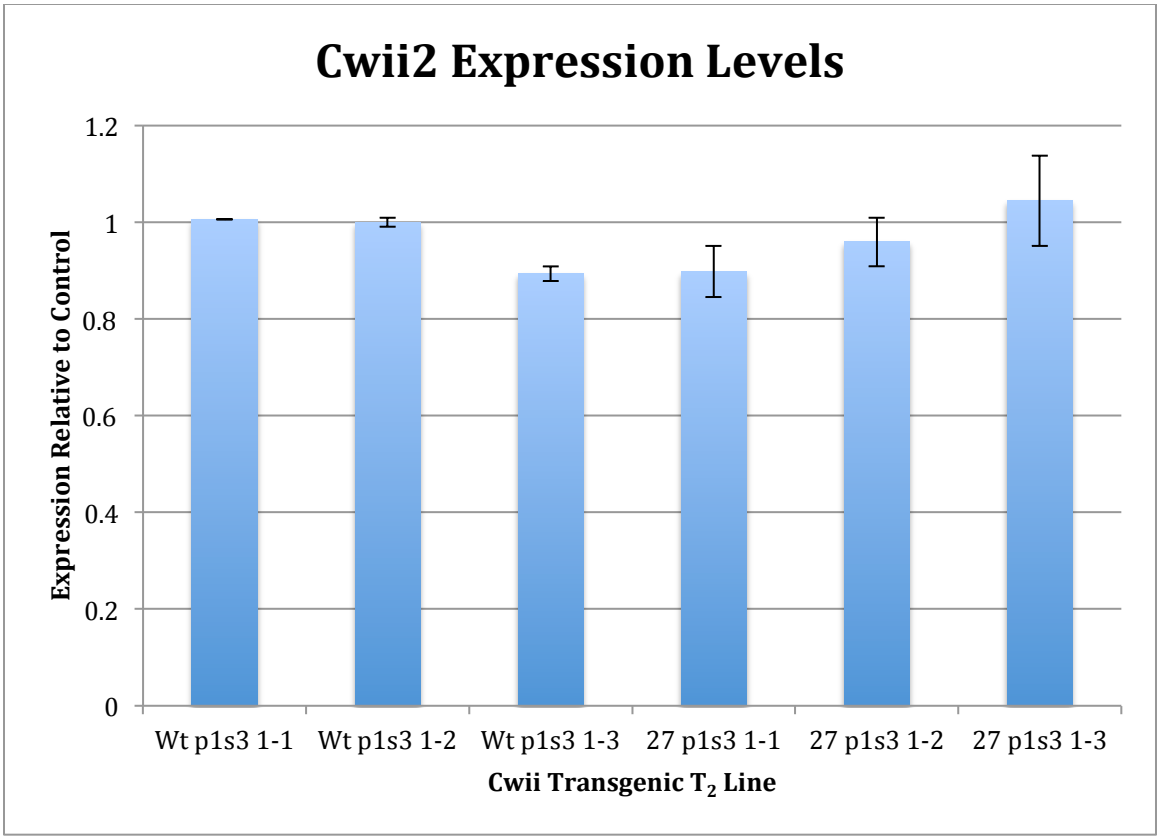

Figure 20: Expression Analysis of Cwii2 in Select T_2 Lines

A graphical representation of Cwii2 expression analysis from select transgenic P1S3 T_2 lines. Error bars represent standard error calculated from a minimum of triplicate reactions.

Based on the expression data calculated for Cwii1 and Cwii2, it appears that Cwii1 shows a decrease in expression, on average, in the selected transgenic T_2 lines. Cwii2 expression doesn't appear to be as affected by the insertion of the RNAi construct. Because the P1S3 Cwii construct contains sequences for both Cwii1 and Cwii2, it is expected that both invertase inhibitors should be down regulated after introduction of the RNAi construct. However, because P1S3 is under control of the Cwii1 native promoter, may explain the cause of a greater effect being seen for Cwii1 expression upon insertion of the P1S3 Cwii RNAi construct.

2.7 T_2 Yield Data

Selected T_2 lines were allowed to reach maturity in the greenhouse and seed was harvested, cleaned and weighed. T_2 seed yield is shown in Figure 21. Two separate plantings of T_2 lines are indicated, and were conducted due to fewer BASTA-resistant T_2s than expected following the initial planting. A second planting increases sample number to decrease statistical error.

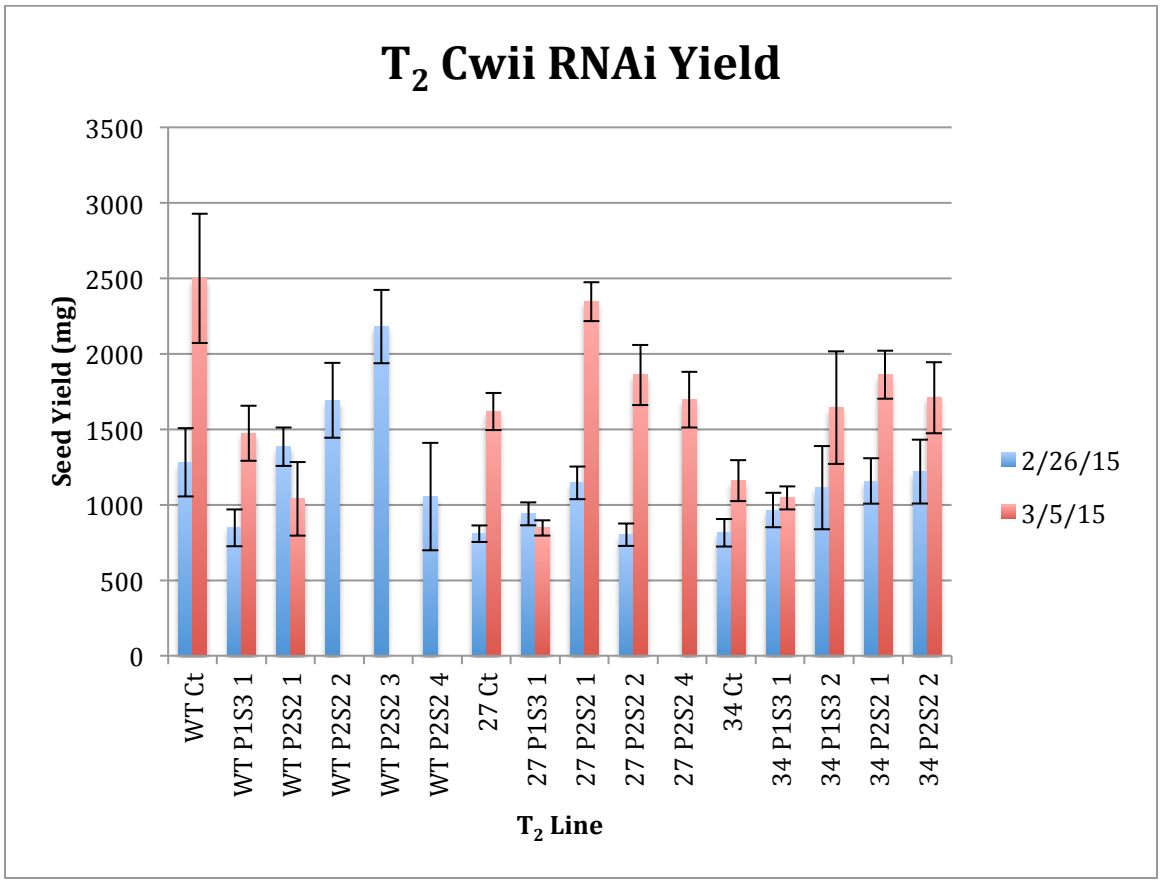

Figure 21: Seed Yield of Select T_2 Lines

A graphical representation of seed yields in milligrams. T_2 yields were clustered by parental T_1s and plotted by harvesting date. The two harvest dates represent two separate plantings of T_2s. The second planting produced larger seed yields on average compared to the first planting. Error bars represent the standard error calculated from a minimum of five biological replicates.

After averaging yields among plants of common parental T_1 lines, yields were analyzed against the parental controls. Figure 22 shows the seed yields of the Cwii RNAi lines relative to the respective parental controls. A value of 1 indicates a level expression consistent with the control, as indicated by the dotted line. This data shows certain T_2 Cwii RNAi lines producing a much greater seed yield relative to controls. LCIA/CCP1 #34 shows a greater increase in seed yield after transgene insertion compared to LCIA/CCP1 #27. This is not an unexpected result, as unpublished data from our laboratory suggests that LCIA/CCP1 #34 exhibits a greater rate of photosynthate production. This means that when increasing photosynthate trafficking to seeds through Cwii RNAi, a greater synergistic effect will be observed on seed yield.

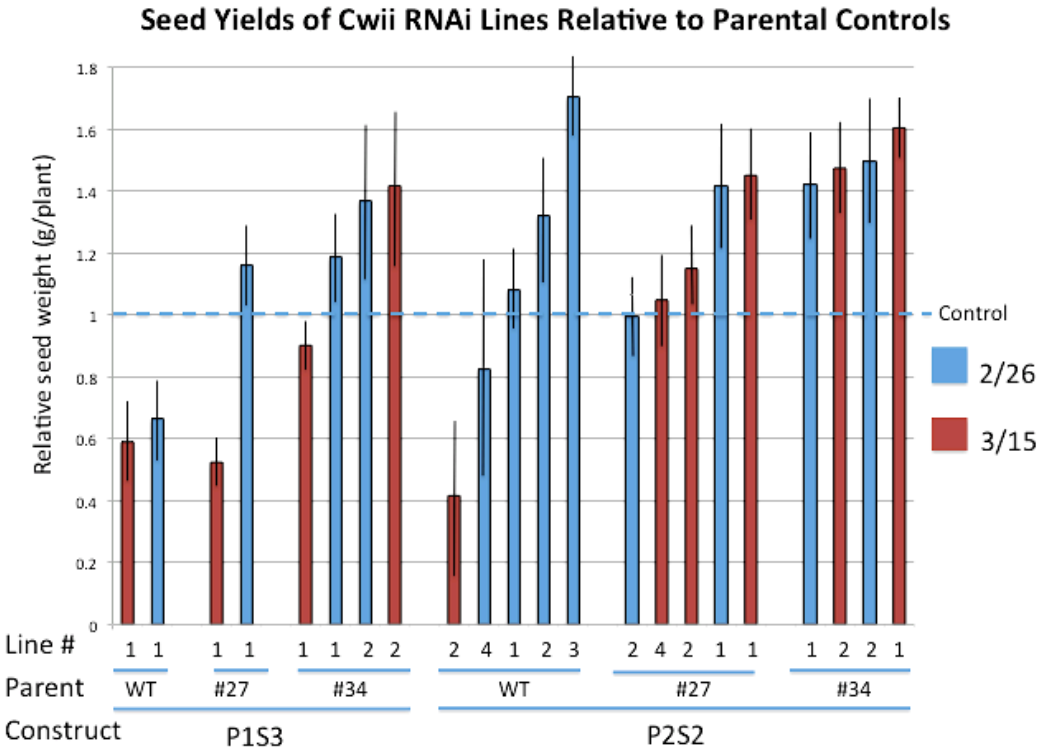

Figure 22: Relative Seed Yield Compared to Parental Controls

A graphical representation of relative seed yields in grams compared to controls of P1S3 and P2S2 Cwii T_2s. The relative control value is set to 1 gram per plant, and is indicated by the dotted blue line, labeled on the left. Error bars represent percent standard deviation of an average of a minimum five biological replicates. Blue bars represent those harvested from the first, 2/26, planting date and red bars represent the second, 3/15, harvesting date. Line numbers and parental background are indicated below the bars.

The P2S2 construct appears to produce a more drastic increase in seed yield relative to expression of the P1S3 Cwii RNAi construct. This may be explained due to P2S2 containing the Cwii2 sequence under control of its native promoter. Recall that Cwii2 is more highly expressed in mature green-leaf tissue, senescing leaves, and developing seed embryos. High invertase activity in source leaves may be implicated in phloem loading. High invertase activity in developing embryos has indicated greater allocation of sucrose and hexoses to the embryo. If Cwii2 were

more effectively silenced in P2S2 backgrounds, a greater allocation of sucrose to the phloem could be expected to result. The increased sucrose presence in the phloem paired with high invertase activity at the sink tissue could result in increased carbon allocation to seed biomass.

CHAPTER 3

3 CONCLUSION

In conclusion it appears that insertion of an RNAi construct designed to inhibit Cwii results in an increase in seed yield relative to parental controls in T_2 transgenics. At the stage we are currently in, further analysis cannot be conducted to compare Cwii RNAi transgenic *C. sativa* with wild type. This is because homozygosity cannot be concluded until screening the T_3 seed by BASTA-selection. Homozygote lines will exhibit a complete resistance to the BASTA herbicide. T_3 lines can then be grown under special growing conditions established by our lab that maximize the increased light conversion efficiency when expressing the LCIA/CCP1 bicarbonate transporters. Through allowing for conditions that maximize the light conversion efficiency, the increased partitioning efficiency achieved through silencing of Cwii with RNAi will result in combined increase on yield potential.

CHAPTER 4

4 MATERIALS & METHODS

4.1 Homology Modeling & Bioinformatics

Sequence alignments were performed using Clustal Omega alignment program. Cell Wall Invertase Inhibitors from tobacco, tomato, potato, and *Arabidopsis thaliana* were selected for alignment. Sequence similarities and identities were noted.

4.2 Cwii RNAi construction

Construction of the plasmid designed for RNAi of Cwii was created through expression of a short silencing RNA hairpin. This was accomplished through inserting a short sense portion of the DNA sequence encoding Cwii, adding in the same sequence in anti-sense conformation following a linker sequence separating the sense and anti-sense sequences. Constructs were made for both Cwii1 and Cwii2, under the control of their own respective promoters. Construct P1S1 expresses the Cwii1 sense and antisense sequences under the control of the Cwii1 native promoter. Construct P2S2 expresses the Cwii2 sense and antisense sequences under the control of the Cwii2 native promoter. Cwii1 and Cwii2 were also made into a single construct under the control of a single promoter, either that of Cwii1 or Cwii2. Construct P1S3 expresses the Cwii1 and Cwii2 sense and antisense sequences under the control of the Cwii1 native promoter. Construct P2S3 expresses the Cwii1 and Cwii2 sense and antisense sequences under the control of the Cwii2 native promoter. The promoter for Cwii1 is natively more expressed in the seed tissue, and the promoter for Cwii2 natively more expressed in the leaves. The RNAi

construct was cloned into vector pEarlyGate301, harboring the BASTA herbicidal resistance and kanamycin bacterial resistance genes.

4.3 *C. sativa* Transformation by Floral Dip

C. sativa were grown in 5-inch pots to flowering, at which point they were transformed using the *Agrobacterium tumefaciens*-mediated transformation by floral dip procedure (Lu & Kang, 2008). Two plants were transformed per pot. Two 1.5 L cultures of *A. tumefaciens* containing the Cwii RNAi construct of interest were grown at 30°C in liquid YEP medium containing the antibiotics rifampicin, gentamycin, and kanamycin for 2 days, or until reaching an appropriate Optical Density was reached. Cells were harvested by centrifugation at low speed to avoid tissue disruption and resuspended in 5% sucrose solution containing silwett. Acetosyringone was added to the solution to induce higher levels or virility. Floral portions of *C. sativa* were submerged in solution and placed in a vacuum desiccator under negative pressure for 7-10 minutes. Dipped plants were allowed to air dry and were staked in vertical positions. Plants reached maturity and were harvested for progeny selection using BASTA.

4.4 Plant Growth Conditions

All plants were grown in an automated greenhouse set for a 16-hour diurnal cycle at 25°C/16°C day/night temperatures. Plants were germinated in moist Pro-mix mycorrhizal soil, contained in 72-well seedling trays. Plants were transplanted after 14 days to 5-inch pots containing soil of the same composition. Plants were maintained by the greenhouse staff and kept at a constantly moist state with intermittent watering including soluble fertilizer. Plants were staked as necessary and allowed to reach full maturity. Upon stem yellowing watering was ceased and plants were allowed to dry and

become fully yellow before harvesting. Harvesting was done in a conventional matter and cleaned using sieves.

4.5 Herbicidal Selection Using BASTA

Positive Cwii transformants were determined using an herbicidal screen with BASTA. T1 seed was planted in standard tray flats in approximately one inch of moist soil and allowed to germinate. After seven days, BASTA herbicide was applied at a concentration of 350 mg/L to the leaves. Approximately 50 milliliters of herbicide was used to treat each flat. This application was repeated after two days. Resistant plants were transplanted to 5-inch pots and allowed to recover from any potential transplant shock, at which point a third BASTA application was applied to further ensure BASTA resistance. T_1 BASTA resistant plants were allowed to mature and T_2 seeds were harvested and collected.

4.6 Genomic PCR Confirmation

Genomic DNA was extracted from BASTA-resistant T_1 transformants using buffer. Eluted into autoclaved water and stored at 4°C. PCR was performed using the Invitrogen GoTaq system. PCR conditions were as followed: Initiation at 95°C for 2 minutes, followed by 35 cycles of 95°C for 30 seconds and annealing at 52.8°C for Cwii1 and 61.7°C for CWii2 for 30 seconds, followed by a 72°C extension for 90 seconds. A final extension at 72°C for 5 minutes and then a 4°C hold was also conducted. PCR products were analyzed on a 1% LE Agarose gel run at 100V in 1X TAE buffer. Invitrogen 1kb-Plus marker was used for a DNA ladder (Cat. No.: 10787-018). Data was visualized with SYBR-Safe DNA Gel stain from Life Technologies (Cat. No.: S33102)

using a 302 nm filter, and imaged using Bio-rad's Molecular Imager Gel Doc XR system and Quantity One software.

4.7 RNA Extraction and cDNA Synthesis

Fresh plant tissues were collected from both leaf and floral tissues. Samples were frozen immediately in liquid nitrogen and maintained at -80° C. RNA extraction and isolation was performed on these frozen samples following the Qiagen RNAeasy Plant Mini Kit procedure (Cat. No.: 74904). Tissue was homogenized in liquid nitrogen using a mortar and pestle. Purity of the RNA was analyzed by light spectrophotometry and gel electrophoresis in 1% LE Agarose. Formaldehyde solution was added to Invitrogen 6X DNA Loading Dye (Cat No.: R0611) to make 5X RNA Loading Dye. First-strand cDNA synthesis was performed using the Invitrogen SuperScript First-Strand Synthesis System for RT-PCR kit (Cat. No.: 11904-018), using 4 ug extracted RNA. The presence of cDNA was confirmed by PCR using primers amplifying the gene *actin*2 .

4.8 RNAi expression analysis

Gene specific Cwii primers were tested on the cDNA to confirm their effectiveness. Semi-quantitative reverse transcript PCR was then performed on the cDNA samples to test for levels of expression of the Cwii gene. Thermo Scientific DyNAmo HS SYBR green qPCR kit was used (Cat. No.: F-410L). Eppendorf RealPlex software and cycler machine was used.

REFERENCES

Agusdinata, D. B., Zhao, F., Ileleji, K., & DeLaurentis, D. (2011). Life cycle assessment of potential biojet fuel production in the united states. *Environmental Science & Technology, 45*(21), 9133-9143.

Ainsworth, E. A., & Rogers, A. (2007). The response of photosynthesis and stomatal conductance to rising [CO2]: Mechanisms and environmental interactions. *Plant, Cell & Environment, 30*(3), 258-270.

Altschul, S. F., Wootton, J. C., Gertz, E. M., Agarwala, R., Morgulis, A., Schäffer, A. A., et al. (2005). Protein database searches using compositionally adjusted substitution matrices. *Febs Journal, 272*(20), 5101-5109.

Altschul, S. F., Madden, T. L., Schaffer, A. A., Zhang, J., Zhang, Z., Miller, W., et al. (1997). Gapped BLAST and PSI-BLAST: A new generation of protein database search programs. *Nucleic Acids Research, 25*(17), 3389-3402.

Amthor, J. S. (2000). The McCree–de Wit–Penning de Vries–Thornley respiration paradigms: 30 years later. *Annals of Botany, 86*(1), 1-20.

Artimo, P., Jonnalagedda, M., Arnold, K., Baratin, D., Csardi, G., de Castro, E., et al. (2012). ExPASy: SIB bioinformatics resource portal. *Nucleic Acids Research, 40*(Web Server issue), W597-603.

Badger, M. R., Kaplan, A., & Berry, J. A. (1980). Internal inorganic carbon pool of chlamydomonas reinhardtii: EVIDENCE FOR A CARBON DIOXIDE-CONCENTRATING MECHANISM. *Plant Physiology, 66*(3), 407-413.

Bate, N. J., Niu, X., Wang, Y., Reimann, K. S., & Helentjaris, T. G. (2004). An invertase inhibitor from maize localizes to the embryo surrounding region during early kernel development. *Plant Physiology, 134*(1), 246-254.

Change, I. C. (1996). The science of climate change. *Second Assessment Report of the Intergovernmental Panel on Climate Change.Cambridge University Press, Cambridge,*

Davenport, C. (2014, June 2, 2014). Obama to take action to slash coal pollution. *New York Times,* pp. A1.

Ellis, R. J. (1979). The most abundant protein in the world. *Trends in Biochemical Sciences, 4*(11), 241-244.

Ellis, R. J. (2010a). Biochemistry: Tackling unintelligent design. *Nature, 463*(7278), 164-165.

Ellis, R. J. (2010b). Biochemistry: Tackling unintelligent design. *Nature, 463*(7278), 164-165.

Giaquinta, R. (1977). Phloem loading of sucrose: pH dependence and selectivity. *Plant Physiology, 59*(4), 750-755.

Goujon, M., McWilliam, H., Li, W., Valentin, F., Squizzato, S., Paern, J., et al. (2010). A new bioinformatics analysis tools framework at EMBL-EBI. *Nucleic Acids Research, 38*(Web Server issue), W695-9.

Greiner, S., Krausgrill, S., & Rausch, T. (1998). Cloning of a tobacco apoplasmic invertase inhibitor. proof of function of the recombinant protein and expression analysis during plant development. *Plant Physiology, 116*(2), 733-742.

Grunden, Michele, A., Sederoff, & Ada, H. (2014). In North Carolina State University Raleigh NC (Ed.), *Synthetic pathway for biological carbon dioxide sequestration* (800/290 ; 424/725; 426/590; 426/615; 426/635; 435/419; 44/307; 554/1; 800/298 ed.). North Carolina: C12N 15/82 20060101 C12N015/82.

Hill, J., Nelson, E., Tilman, D., Polasky, S., & Tiffany, D. (2006). Environmental, economic, and energetic costs and benefits of biodiesel and ethanol biofuels. *Proceedings of the National Academy of Sciences of the United States of America, 103*(30), 11206-11210.

Hothorn, M., D'Angelo, I., Marquez, J. A., Greiner, S., & Scheffzek, K. (2004). The invertase inhibitor nt-CIF from tobacco: A highly thermostable four-helix bundle with an unusual N-terminal extension. *Journal of Molecular Biology, 335*(4), 987-995.

Hothorn, M., Van den Ende, W., Lammens, W., Rybin, V., & Scheffzek, K. (2010). Structural insights into the pH-controlled targeting of plant cell-wall invertase by a specific inhibitor protein. *Proceedings of the National Academy of Sciences of the United States of America, 107*(40), 17427-17432.

Huala, E., Dickerman, A. W., Garcia-Hernandez, M., Weems, D., Reiser, L., LaFond, F., et al. (2001). The arabidopsis information resource (TAIR): A comprehensive database and web-based information retrieval, analysis, and visualization system for a model plant. *Nucleic Acids Research, 29*(1), 102-105.

Jin, Y., Ni, D. A., & Ruan, Y. L. (2009). Posttranslational elevation of cell wall invertase activity by silencing its inhibitor in tomato delays leaf senescence and increases seed weight and fruit hexose level. *The Plant Cell, 21*(7), 2072-2089.

Kagale, S., Koh, C., Nixon, J., Bollina, V., Clarke, W. E., Tuteja, R., et al. (2014). The emerging biofuel crop camelina sativa retains a highly undifferentiated hexaploid genome structure. *Nature Communications, 5*, 3706.

Koch, K. (2004). Sucrose metabolism: Regulatory mechanisms and pivotal roles in sugar sensing and plant development. *Current Opinion in Plant Biology, 7*(3), 235-246.

Krausgrill, S., Sander, A., Greiner, S., Weil, M., & Rausch, T. (1996). Regulation of cell wall invertase by a proteinaceous inhibitor. *Journal of Experimental Botany, 47 Spec No*, 1193-1198.

Larkin, M. A., Blackshields, G., Brown, N. P., Chenna, R., McGettigan, P. A., McWilliam, H., et al. (2007). Clustal W and clustal X version 2.0. *Bioinformatics (Oxford, England), 23*(21), 2947-2948.

Leakey, A. D., Ainsworth, E. A., Bernacchi, C. J., Rogers, A., Long, S. P., & Ort, D. R. (2009). Elevated CO2 effects on plant carbon, nitrogen, and water relations: Six important lessons from FACE. *Journal of Experimental Botany, 60*(10), 2859-2876.

Leakey, A. D., Xu, F., Gillespie, K. M., McGrath, J. M., Ainsworth, E. A., & Ort, D. R. (2009). Genomic basis for stimulated respiration by plants growing under elevated carbon dioxide. *Proceedings of the National Academy of Sciences of the United States of America, 106*(9), 3597-3602.

Ledley, T. S., Sundquist, E. T., Schwartz, S. E., Hall, D. K., Fellows, J. D., & Killeen, T. L. (1999). Climate change and greenhouse gases. *Eos, Transactions American Geophysical Union, 80*(39), 453-458.

Li, P., Ainsworth, E. A., Leakey, A. D., Ulanov, A., Lozovaya, V., Ort, D. R., et al. (2008). Arabidopsis transcript and metabolite profiles: Ecotype-specific responses to open-air elevated [CO2]. *Plant, Cell & Environment, 31*(11), 1673-1687.

Li, X., & Mupondwa, E. (2014). Life cycle assessment of camelina oil derived biodiesel and jet fuel in the canadian prairies. *Science of the Total Environment, 481*(0), 17-26.

Li, Y., Xu, J., Haq, N. U., Zhang, H., & Zhu, X. G. (2014). Was low CO2 a driving force of C4 evolution: Arabidopsis responses to long-term low CO2 stress. *Journal of Experimental Botany, 65*(13), 3657-3667.

Lin, M. T., Occhialini, A., Andralojc, P. J., Parry, M. A., & Hanson, M. R. (2014). A faster rubisco with potential to increase photosynthesis in crops. *Nature, 513*(7519), 547-550.

Long, S. P., Ainsworth, E. A., Rogers, A., & Ort, D. R. (2004). Rising atmospheric carbon dioxide: Plants FACE the future*. *Annu.Rev.Plant Biol., 55*, 591-628.

Long, S. P., ZHU, X., Naidu, S. L., & Ort, D. R. (2006). Can improvement in photosynthesis increase crop yields? *Plant, Cell & Environment, 29*(3), 315-330.

Lu, C., & Kang, J. (2008). Generation of transgenic plants of a potential oilseed crop camelina sativa by agrobacterium-mediated transformation. *Plant Cell Reports, 27*(2), 273-278.

Maclean, I. M., & Wilson, R. J. (2011). Recent ecological responses to climate change support predictions of high extinction risk. *Proceedings of the National Academy of Sciences of the United States of America, 108*(30), 12337-12342.

Marland, G., Boden, T. A., Andres, R. J., Brenkert, A., & Johnston, C. (2003). Global, regional, and national fossil fuel CO2 emissions. *Trends: A Compendium of Data on Global Change,* , 34-43.

Monteith, J., & Moss, C. (1977). Climate and the efficiency of crop production in britain [and discussion]. *Philosophical Transactions of the Royal Society B: Biological Sciences, 281*(980), 277-294.

Moroney, J. V., Ma, Y., Frey, W. D., Fusilier, K. A., Pham, T. T., Simms, T. A., et al. (2011). The carbonic anhydrase isoforms of chlamydomonas reinhardtii: Intracellular location, expression, and physiological roles. *Photosynthesis Research, 109*(1-3), 133-149.

Price, G. D., Badger, M. R., & von Caemmerer, S. (2011). The prospect of using cyanobacterial bicarbonate transporters to improve leaf photosynthesis in C3 crop plants. *Plant Physiology, 155*(1), 20-26.

Putnam, D., Budin, J., Field, L., & Breene, W. (1993). Camelina: A promising low-input oilseed. *New Crops.Wiley, New York, 314*

Rausch, T., & Greiner, S. (2004). Plant protein inhibitors of invertases. *Biochimica Et Biophysica Acta, 1696*(2), 253-261.

Rolland, F., Baena-Gonzalez, E., & Sheen, J. (2006). Sugar sensing and signaling in plants: Conserved and novel mechanisms. *Annual Review of Plant Biology, 57*, 675-709.

Scognamiglio, M. A., Ciardiello, M. A., Tamburrini, M., Carratore, V., Rausch, T., & Camardella, L. (2003). The plant invertase inhibitor shares structural properties and disulfide bridges arrangement with the pectin methylesterase inhibitor. *Journal of Protein Chemistry, 22*(4), 363-369.

Sherson, S. M., Alford, H. L., Forbes, S. M., Wallace, G., & Smith, S. M. (2003). Roles of cell-wall invertases and monosaccharide transporters in the growth and development of arabidopsis. *Journal of Experimental Botany, 54*(382), 525-531.

Shonnard, D. R., Williams, L., & Kalnes, T. N. (2010). Camelina-derived jet fuel and diesel: Sustainable advanced biofuels. *Environmental Progress & Sustainable Energy, 29*(3), 382-392.

Sonnewald, U., Hajirezaeiz, M., Kossmannm, J., Heyerm, A., Trethewey, R. N., & Willmitzer, L. (1997). Increased potato tuber size resulting from apoplastic expression of. *Nature Biotechnology, 15*

Spreitzer, R. J., & Salvucci, M. E. (2002). Rubisco: Structure, regulatory interactions, and possibilities for a better enzyme. *Annual Review of Plant Biology, 53*(1), 449-475.

Sturm, A. (1999). Invertases. primary structures, functions, and roles in plant development and sucrose partitioning. *Plant Physiology, 121*(1), 1-8.

Thomas, C. D., Cameron, A., Green, R. E., Bakkenes, M., Beaumont, L. J., Collingham, Y. C., et al. (2004). Extinction risk from climate change. *Nature, 427*(6970), 145-148.

von Caemmerer, S., Quick, W. P., & Furbank, R. T. (2012). The development of C(4)rice: Current progress and future challenges. *Science (New York, N.Y.), 336*(6089), 1671-1672.

Wang, J., Nayak, S., Koch, K., & Ming, R. (2013). Carbon partitioning in sugarcane (saccharum species). *Frontiers in Plant Science, 4*

Wang, L., & Ruan, Y. L. (2012). New insights into roles of cell wall invertase in early seed development revealed by comprehensive spatial and temporal expression patterns of GhCWIN1 in cotton. *Plant Physiology, 160*(2), 777-787.

Wang, Y., & Spalding, M. H. (2014). Acclimation to very low CO2: Contribution of limiting CO2 inducible proteins, LCIB and LCIA, to inorganic carbon uptake in chlamydomonas reinhardtii. *Plant Physiology, 166*(4), 2040-2050.

Williams, J. H., & Farrar, J. F. (1990). Control of barley root respiration. *Physiologia Plantarum, 79*(2), 259-266.

Winter, D., Vinegar, B., Nahal, H., Ammar, R., Wilson, G. V., & Provart, N. J. (2007). An "Electronic fluorescent pictograph" browser for exploring and analyzing large-scale biological data sets. *PloS One, 2*(8), e718.

Zhu, X., Long, S. P., & Ort, D. R. (2010). Improving photosynthetic efficiency for greater yield. *Annual Review of Plant Biology, 61*, 235-261.